

# Journal Pre-proof

Fate and transport of ten plant protection products of emerging concern in a coastal lagoon: application and evaluation of a multimedia level III fugacity model

Loris Calgaro, Elisa Giubilato, Lara Lamon, Elena Semenzin, Antonio Marcomini



PII: S0013-9351(24)01954-6

DOI: <https://doi.org/10.1016/j.envres.2024.120047>

Reference: YENRS 120047

To appear in: *Environmental Research*

Received Date: 2 February 2024

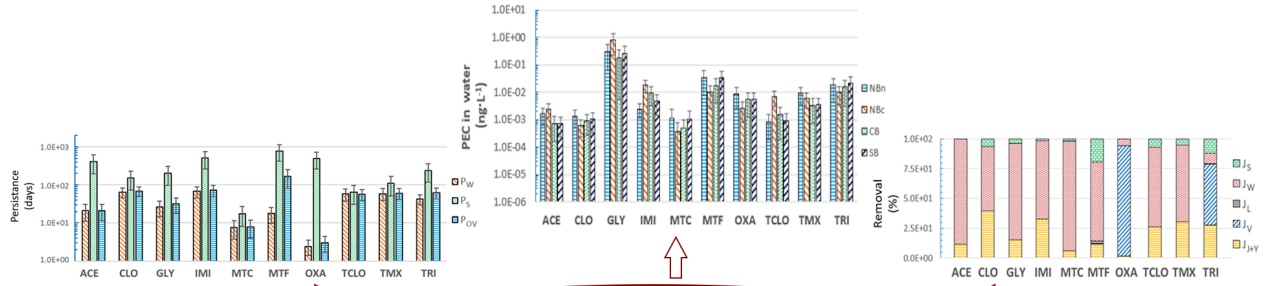
Revised Date: 1 August 2024

Accepted Date: 20 September 2024

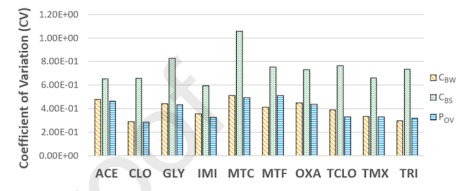
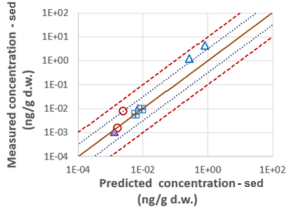
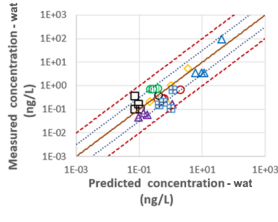
Please cite this article as: Calgaro, L., Giubilato, E., Lamon, L., Semenzin, E., Marcomini, A., Fate and transport of ten plant protection products of emerging concern in a coastal lagoon: application and evaluation of a multimedia level III fugacity model, *Environmental Research*, <https://doi.org/10.1016/j.envres.2024.120047>.

This is a PDF file of an article that has undergone enhancements after acceptance, such as the addition of a cover page and metadata, and formatting for readability, but it is not yet the definitive version of record. This version will undergo additional copyediting, typesetting and review before it is published in its final form, but we are providing this version to give early visibility of the article. Please note that, during the production process, errors may be discovered which could affect the content, and all legal disclaimers that apply to the journal pertain.

© 2024 Published by Elsevier Inc.



**Level III multimedia model**



Journal Pre-proof

# Fate and transport of ten plant protection products of emerging concern in a coastal lagoon: application and evaluation of a multimedia level III fugacity model

Loris Calgaro<sup>1\*</sup>, Elisa Giubilato<sup>1</sup>, Lara Lamon<sup>1</sup>, Elena Semenzin<sup>1</sup>, Antonio Marcomini<sup>1</sup>

<sup>1</sup>Department of Environmental Sciences, Informatics and Statistics, University Ca' Foscari of Venice, Via Torino 155, 30172 Venice Mestre, Italy.

[loris.calgaro@unive.it](mailto:loris.calgaro@unive.it) (L.C.); [lara.lamon@unive.it](mailto:lara.lamon@unive.it) (L.L.); [giubilato@unive.it](mailto:giubilato@unive.it) (E.G.); [semenzin@unive.it](mailto:semenzin@unive.it) (E.S.); [marcom@unive.it](mailto:marcom@unive.it) (A.M.)

\*Corresponding author: Loris Calgaro

E-mail: [loris.calgaro@unive.it](mailto:loris.calgaro@unive.it)

Address: Department of Environmental Sciences, Informatics and Statistics,  
University Ca' Foscari of Venice, Via Torino 155, 30172 Venice Mestre,  
Italy

## Abstract

Multimedia fugacity models are effective tools for studying the environmental behaviour and occurrence of contaminants of emerging concern (CECs) and assessing associated risks, especially when experimental data is limited. These models describe processes controlling chemical partitioning, transport, and reactions in environmental media using mathematical statements based on the concept of fugacity.

To aid in identifying and prioritizing CECs for future local monitoring, we present here the application of a level III multimedia fugacity model assuming non-equilibrium between compartments and steady-state conditions. This model estimated predicted environmental concentrations (PECs), persistence, distribution, and transport of ten plant protection products (PPPs) in the Venice Lagoon, a complex coastal environment under high anthropogenic pressure.

The model was evaluated through uncertainty and sensitivity analysis using the Monte Carlo approach and by comparing PECs with PPP concentrations measured during four sampling campaigns. Results showed good agreement with field data, with the highest concentrations in water and sediments estimated for glyphosate, followed by imidacloprid, metaflumizone, and triallate. The model indicated accumulation of all investigated PPPs in sediments. For most chemicals, advection outflow and degradation in the water column were the main removal mechanisms, while volatilization was significant only for oxadiazon and triallate.

Sensitivity and uncertainty analysis revealed that degradation rates, organic carbon/water partitioning coefficients ( $K_{OC}$ ), and parameters describing air-water interactions had the strongest influence on the model's results, followed by inputs accounting for sediment sinking and resuspension. The lack of data on PPP degradation in brackish waters accounted for most of the uncertainty in model results.

This work shows how a relatively simple multimedia model can offer new insights into the environmental behaviour of PPPs in a complex transitional waterbody such as the Venice lagoon, providing useful data for the identification of the CECs to be prioritised in future local monitoring efforts.

## 41 **Keywords**

42 Emerging contaminants, Environmental pollution, Venice Lagoon, Plant protection products, Exposure and risk  
43 assessment.

## 44 **Highlights**

- 45 • The first multimedia modelling of plant protection products in the Venice Lagoon
- 46 • Concentration and environmental fate of ten plant protection products were simulated
- 47 • The highest modelled and measured concentration in water and sediments was of glyphosate and  
48 imidacloprid
- 49 • The study provides data to support ecological risk assessment for the Venice Lagoon
- 50 • Degradation rates, partitioning coefficients, and air-water interactions had strong effects on model  
51 results

## 52 **1. Introduction**

53 Water pollution has been widely recognized as a severe worldwide problem (Geissen et al., 2015), due to a  
54 multitude of contaminants detected across the world's water bodies (Sharma and Bhattacharya, 2017). For  
55 several decades, the attention of the scientific community has been focused on conventional pollutants, which  
56 include many compounds whose high environmental persistence is linked to their lipophilicity and stability,  
57 such as polychlorinated biphenyls (PCBs), polycyclic aromatic hydrocarbons (PAHs), polychlorinated  
58 dibenzodioxins and furans (PCDDs/PCDFs), and pesticides (Calza et al., 2013). In more recent years, thanks to  
59 the development of improved methods of detection, identification, and quantification of organic substances in  
60 many environmental media (Stefanakis and Becker, 2015), the presence in several environmental compartments  
61 of many "contaminants of emerging concern" (CECs) has been brought to attention. In detail, CECs are defined  
62 as "synthetic or naturally occurring chemicals that are not commonly monitored in the environment but which  
63 have the potential to enter the environment and cause known or suspected adverse ecological and (or) human  
64 health effects" (Geissen et al., 2015). The release to the environment of these contaminants may have occurred  
65 for a long time (e.g. wastewater treatment, agriculture, and industry), but it may not have been recognized until  
66 sufficient detection methods were developed. In other cases, both the synthesis of new chemicals or changes in  
67 the use and disposal of existing chemicals could have created new sources of these substances (NORMAN,  
68 2020). In this context, more than 700 compounds (i.e. CECs, their transformation products, and their  
69 metabolites) have been detected in surface waters, groundwater, and marine waters (Geissen et al., 2015).

70 In particular, plant protection products (PPPs) have been widely recognized to have adverse impacts on both  
71 the environment and human health. The presence in the environment of such chemicals can be attributed to  
72 several phenomena, such as leaching into groundwater, surface run-off, and drift into non-target areas (Lupi et  
73 al., 2019), leading to acute and chronic (e.g., neurotoxicity, immunotoxicity, endocrine disruption, and  
74 behavioural changes) negative effects for both soil-dwelling (e.g. earthworms and microorganisms) and non-  
75 soil dwelling (e.g. molluscs, fish, pollinators, birds, and larger mammals) organisms (Christen et al., 2018;  
76 Pogăcean and Gavrilesco, 2009). Furthermore, plant protection residues on food and in drinking water have  
77 been identified among the main factors leading to human exposure (FAO and ITPS, 2017).

78 In these circumstances protecting water quality becomes of fundamental importance to minimize environmental  
79 and human risk, therefore starting from the EU 2000/60/EC directive (European Commission, 2000), several  
80 actions have been undertaken by the European Union for a better management of hydric resources. Within this  
81 framework, due to the potential impact that these substances may have on ecosystem and human health, the lack  
82 of knowledge regarding their behaviour in the environment and the deficiency in analytical and sampling

83 techniques (Geissen et al., 2015), the need of detailed ecological risk assessment (ERA) evaluations for these  
84 substances has been widely recognized (Stefanakis and Becker, 2015).

85 Among the available tools to carry out these evaluations, the use of models has been identified as a reliable low-  
86 cost tool for estimating, identifying, and managing environmental and ecological risks (Şimşek et al., 2019).  
87 The models used within this framework may vary in relation to their purpose, scope, and level of analysis. In  
88 particular, the models used during different stages of the ERA process include fate-exposure models, exposure-  
89 effect models, and integrated models (Vaz, 2019).

90 Fate-exposure models cover the first half of the source-to-outcome continuum (Williams et al., 2010) and  
91 simulate the transport and transformation of pollutants in the environment to predict the concentrations of these  
92 substances in different environmental media (e.g., atmosphere, water, soil, and sediments) (Vaz, 2019). Since  
93 the results of these models represent concentrations to which target organisms could be potentially exposed, this  
94 data is often used instead of measured concentrations as an input to exposure-effect models, which are applied  
95 in the final part of the source-to-outcome continuum of the ERA (Vaz, 2019).

96 One of the most used approaches used to develop multimedia fate models is to describe the processes controlling  
97 chemical partitioning and reactions in the environment by developing and applying mass balance equations  
98 based on the concept of fugacity developed by Mackay and co-workers (Mackay et al., 1985, 1983a; Mackay  
99 and Diamond, 1989). These equations are solved combining information regarding environmental  
100 compartments characteristics, chemicals' emissions, transport and elimination processes, in order to estimate  
101 the distribution and concentrations of the target substances in each media of the modelled system (Mackay and  
102 Paterson, 1991), provide a quantitative analysis of the emission sources, transport and transfer routes, as well  
103 as estimate where contaminants may accumulate within the system under investigation (MacLeod et al., 2010;  
104 Su et al., 2019; Vaz, 2019; Wang et al., 2020a).

105 Multimedia fugacity model models can be set-up considering different levels of complexity depending on the  
106 specific requirements of the study, data availability, and the desired accuracy of predictions. In particular,  
107 fugacity models considering i) adjective and diffusive (both intra- and inter-media) transport processes, ii) non-  
108 equilibrium conditions between different compartments, and iii) steady state mass-balance (i.e., level III  
109 fugacity models) are one of the most diffused multimedia fugacity models (Wang et al., 2020b), which have  
110 been applied to investigate the fate of a multitude of both conventional (e.g., DDT, PCBs, and PAHs) (Fang et  
111 al., 2016; Mackay and Diamond, 1989; Xu et al., 2013) and CECs (e.g., pharmaceuticals, herbicides, and  
112 hormones) (Tan et al., 2007; Wang et al., 2020b) within several environmental systems such as rivers, lakes,  
113 estuaries, wetlands, catchments, and lagoons (Cancelli et al., 2019; Fang et al., 2016; Kilic and Aral, 2009;  
114 Mugnai et al., 2010; Warren et al., 2005).

115 This study aimed to simulate, using a multimedia level III fugacity model, the environmental fate and  
116 distribution of ten PPPs in the Lagoon of Venice with the objective of improving the understanding about the  
117 processes governing their environmental behaviour, especially those involved in their natural attenuation.  
118 Moreover, this work aimed at estimating the exposure of lagoon ecosystems to these chemicals to support future  
119 risk assessment efforts, in particular to facilitate the identification of priority contaminants for the case study  
120 area to be included into dedicated future monitoring campaigns.

## 121 **2. Materials and methods**

### 122 **2.1 Study area**

123 The lagoon of Venice (Figure 1b) is the largest transitional water body in the Adriatic Sea and it is composed  
124 by a complex ensemble of aquatic and terrestrial environments, covering a half-moon shaped area of about 550  
125 km<sup>2</sup> (Umgiesser et al., 2004). The prevailing direction of the wind is NE–SW and water temperature ranges  
126 from 0 to 30 °C (Umgiesser et al., 2004). Its drainage basin is situated in a highly populated area (ca. 635  
127 people/km<sup>2</sup>) (ISTAT, 2012; Veneto Region, 2020a), corresponding to about 1600 inhabitant equivalents per  
128 km<sup>2</sup> if industrial and agricultural activities are also taken into account (Dalla Valle et al., 2003). This causes the

129 lagoon's ecosystem to be subjected to several pressures due to numerous stressors such as contaminant loadings  
 130 from transports, industry, agriculture, human settlements, and fishing activities.

131 The lagoon is mainly composed of a mix of shallow waters with an average depth of about 1 m and mudflats,  
 132 which is crossed by a complex system of channels (maximum depth > 15 m) (Ferrarin et al., 2019), thus creating  
 133 a quite complex hydrological system. The lagoon has been subdivided into four main basins (NBn, NBc, CB,  
 134 and SB) according to modelled hydro-dynamic circulation patterns (Solidoro et al., 2004) considering the three  
 135 inlets (Lido, Malamocco, and Chioggia) that allow water exchange with the Adriatic Sea (Dalla Valle et al.,  
 136 2003) and the freshwater inflow from 12 major tributaries, whose drainage basin covers an area of about 2530  
 137 km<sup>2</sup> (Veneto Region, 2020a). In detail, the subdivision of the Venice lagoon and the average net flows of water  
 138 (m<sup>3</sup>/s) to and from each segment are reported in Figure 1b.

139

## 140 2.2 Target plant protection products and emission inventory

141 Ten PPPs (i.e. methiocarb (MTC), metaflumizone (MTF), and glyphosate (GLY), oxadiazon (OXA), triallate  
 142 (TRI), imidacloprid (IMI), thiacloprid (TCLO), thiamethoxam (TMX), clothianidin (CLO), and acetamiprid  
 143 (ACE)) were selected for this study after a review of the existing knowledge on CECs in Europe, Italy and the  
 144 lagoon of Venice and its watershed, considering also the two versions of the Watch List already established  
 145 when this work was planned (i.e., DIR 2015/495 EU and DIR 2018/840 EU (European Commission, 2015;  
 146 European Commission, 2018)).

147 Mean emission rates in each region of the Venice lagoon drainage basin for the target chemicals were calculated  
 148 starting from PPPs annual sales data by applying the approach reported in a previous work (Calgaro et al., 2023).  
 149 In some detail, we assumed the use and release into the environment of the studied PPPs to be proportional to  
 150 the area dedicated to agriculture present in each of the lagoon drainage sub-basins. These areas were estimated  
 151 by GIS-based spatial analysis of the Veneto Region land-use census map of 2018 (Veneto Region, 2020b) and  
 152 of the shapefiles reporting the confines of each of the lagoon's sub-regions drainage basin (Veneto Region,  
 153 2019).

154 Finally, concentration of each PPP in the riverine inflow water of each sub-basin ( $C_{IW}$ , ng·L<sup>-1</sup>) was calculated  
 155 by applying Eq. 1 (Table S1):

$$C_{IW} = [(E_{PPP_i}) / (J_I \cdot 8760 h)] \cdot 10^9 \quad \text{Eq. 1}$$

156 where  $E_{PPP_i}$  (kg·year<sup>-1</sup>) is the annual average emission of the target PPPs to each sub-area of the Venice lagoon  
 157 drainage basin, and  $J_I$  (m<sup>3</sup>·h<sup>-1</sup>) is the corresponding average annual riverine input (Solidoro et al., 2004). Since  
 158 there is no significant cropland within the Venice lagoon, we assumed that no direct emission of PPPs was  
 159 present (i.e.  $E_W = 0$ ). Also, we assumed that no adjective inflow of the target chemicals in the air occurred for  
 160 the Venice lagoon due to their low volatility (EPPO, 2003) or quick removal from the atmosphere after  
 161 application by wet deposition (Chang et al., 2011; Messing et al., 2011; Ravier et al., 2019).

## 162 2.3 Modelling approach

### 163 2.3.1 Model description

164 A multimedia level III fugacity model based on the approaches of Mackay and colleagues (Mackay et al., 1983a,  
 165 1983b; Mackay and Diamond, 1989; Mackay and Paterson, 1991) was set-up to investigate the distribution and  
 166 fate of several plant protection products in the lagoon of Venice.

167 The conceptual diagram of the model presented in Figure 1a shows that air, water, and sediment were defined  
 168 as three bulk compartments, while six additional sub-compartments were included in the three bulk  
 169 compartments as follows: i) air, and particles in the air, ii) water, and suspended solids in water, iii) pore water  
 170 and solids in sediment. The processes taken into consideration are shown in Figure 1a, while additional details  
 171 are given in paragraph 2.3.2.

172 Similarly to Sommerfreund and co-workers (2010a, b) (Sommerfreund et al., 2010b, 2010a), we focused our  
 173 modelling exercise on the sub-basins of the Venice Lagoon (NBn, NBc, CB, and SB) defined by Solidoro et al.  
 174 (2004) and shown in b, using the reference scenario of “no wind” to represent the steady-state hydrologic  
 175 circulation pattern of the lagoon (Solidoro et al., 2004). In particular, water flow between each sub-basin was  
 176 considered as a unidirectional net flux having the same concentration in the water of suspended particle matter  
 177 (SPM) and contaminant of the stating water body, while no transfer of sediment between sub-basins was  
 178 contemplated in the model.  
 179

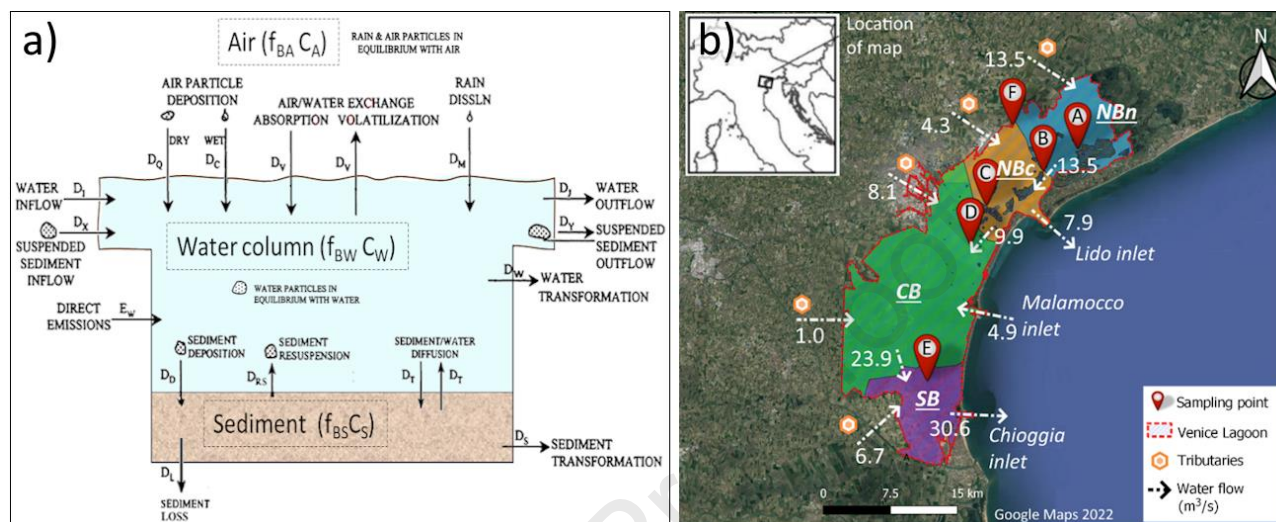


**Figure 1:** a) Transport and transformation processes treated in the multimedia level III fugacity model, consisting of a defined atmosphere with water and sediment compartments. Adapted from Mackay et al. (2001); b) Subdivision of the Venice Lagoon into four main basins (i.e., NBn, NBc, CB, and SB) according to modelled hydro-dynamic circulation patterns. Red symbols denote the selected sampling points, while arrows indicate average annual flows of water expressed as  $m^3/s$ . Adapted from Solidoro et al. (2004) and Sommerfreund et al. (2010b).

180

181 The concentrations of the target chemicals in each compartment and the transfer fluxes between adjacent  
 182 compartments and sub-basins were modelled under a steady-state assumption by using a MS Excel version of  
 183 a multimedia level III fugacity model, as reported by Mackay and co-workers (Mackay et al., 2014).

184 The model calculates the predicted environmental concentration (PEC) of the target chemical in each  
 185 compartment based on the linear relationship between fugacity ( $f$ , Pa) and concentration ( $C$ ,  $mol/m^3$ ), as shown  
 186 in Eq. 2.

$$C = Z \cdot f \quad \text{Eq. 2}$$

187 Where  $Z$  (fugacity capacity,  $mol \cdot m^{-3} \cdot Pa^{-1}$ ) is a proportionality constant dependent on the temperature, on the  
 188 nature of the compartment and the physical-chemical properties of the compound. In detail,  $Z$  values are  
 189 calculated from the relationships reported in Table 1 (Mackay, 2001).

190

**Table 1.** Fugacity capacities ( $Z$ ,  $\text{mol}\cdot\text{m}^{-3}\cdot\text{Pa}^{-1}$ ) and D values (D values,  $\text{mol}\cdot\text{Pa}^{-1}\cdot\text{h}^{-1}$ ) for each segment of the level III multimedia fugacity model to calculate intermedia and reaction rates and the corresponding multiplying fugacity used to calculate each process' flux (Franco and Trapp, 2010; Mackay, 2001).

Process	D value	Definition of D Value	Multiplying Fugacity	Fugacity capacity
Volatilization	$D_V$	$\left[ K_{AW} / \left( \frac{K_{AW}}{k_{VW}} + \frac{1}{k_{VA}} \right) \right] \cdot A_W \cdot (1/H) \cdot$	$f_W$	$Z_{BA} = Z_A \cdot f_A + Z_Q \cdot f_Q$
Adsorption	$D_V$	$\left[ K_{AW} / \left( \frac{K_{AW}}{k_{VW}} + \frac{1}{k_{VA}} \right) \right] \cdot A_W \cdot (1/H) \cdot$	$f_A$	$Z_A = 1/RT$
Rain dissolution	$D_M$	$G_M \cdot Z_W \cdot$	$f_A$	$Z_Q = (1/RT) \cdot [(6 \cdot 10^6)/P^V]$
Wet particle deposition	$D_C$	$G_C \cdot Z_Q \cdot$	$f_A$	$Z_{BW} = [Z_W \cdot (1 - f_P)] + (Z_P f_P)$
Dry particle deposition	$D_Q$	$G_Q \cdot Z_Q \cdot$	$f_A$	$Z_W = [(1/H) \cdot (I + 1)]$
Sediment deposition	$D_D$	$G_D \cdot Z_P \cdot$	$f_W$	$Z_P = K_{OC-P} \cdot \rho_P \cdot Z_W \cdot f_{OC-P}/H$
Sediment resuspension	$D_{RS}$	$G_{RS} \cdot Z_S \cdot$	$f_S$	$Z_{BIW} = [Z_{IW} \cdot (1 - f_{IP})] + (Z_{IP} f_{IP})$
Sediment to water diffusion	$D_T$	$k_T \cdot A_S \cdot Z_W$	$f_S$	$Z_{IW} = [(1/H) \cdot (I + 1)]$
Water to sediment diffusion	$D_T$	$k_T \cdot A_S \cdot Z_W$	$f_W$	$Z_{IP} = K_{OC-IP} \cdot \rho_{IP} \cdot Z_{IW} \cdot f_{OC-IP}/H$
Water inflow	$D_I$	$G_I \cdot Z_W$	$f_I$	$Z_{BS} = [Z_{SPW} \cdot (1 - f_S)] + (Z_S f_S)$
Water particle inflow	$D_X$	$G_R \cdot Z_P$	$f_I$	$Z_{SPW} = [(1/H) \cdot (I + 1)]$
Sediment loss	$D_L$	$G_L \cdot Z_S$	$f_S$	$Z_S = K_{OC-S} \cdot \rho_S \cdot Z_W$
Sediment transformation	$D_S$	$k_S \cdot V_S \cdot Z_S$	$f_S$	$Z_{RS} = K_{OC-RS} \cdot \rho_S / 1000$
Water transformation	$D_W$	$k_W \cdot V_W \cdot Z_W$	$f_W$	$Z_M = [(1/H) \cdot (I + 1)]$
Water outflow	$D_J$	$G_J \cdot Z_W$	$f_W$	
Water particle outflow	$D_Y$	$G_Y \cdot Z_P$	$f_W$	
Direct emissions in water	–	$E_W$	–	

Subscripts indicate the environmental compartment corresponding each parameter: BA = bulk air, A = air gas phase, Q = air particulate, BW = bulk water, W = water, P = particulate matter in water, BIW = bulk inflow water, IW = inflow water, IP = particulate matter in inflow water, BS = bulk sediment, S = sediment solids, SPW = sediment pore water, RS = resuspended sediment, and M = rain. R = ideal gas constant ( $J\cdot\text{mol}^{-1}\cdot\text{K}^{-1}$ );  $P^V$  = vapour pressure (Pa);  $\rho$  = density ( $\text{kg}\cdot\text{m}^{-3}$ );  $K_{OC}$  = organic carbon–water partition coefficient;  $f_{OC}$  = organic carbon fraction;  $f$  = volume fraction.  $k_S$  and  $k_W$  are transformation rate constants ( $\text{h}^{-1}$ ) for sediment and water, respectively.  $k_T$  is a sediment–water mass transfer coefficient ( $\text{m}\cdot\text{h}^{-1}$ ) while  $k_{VW}$  and  $k_{VA}$  are overall the water–side and air–water mass transfer coefficients ( $\text{m}\cdot\text{h}^{-1}$ ), respectively.  $A_W$  and  $A_S$  are the air–water and water–sediment interfaces area ( $\text{m}^2$ ), respectively.  $V_W$  and  $V_S$  are water and sediment volumes ( $\text{m}^3$ ).  $K_{AW}$  is the air–water partition coefficient. For additional details see Table S2, Table S3, and Table S4.



192 The Henderson-Hasselbalch relationship was used to calculate the ratio of ionic to non-ionic forms (I) for the  
 193 target chemicals that dissociate in the water (Mackay, 2001) (i.e. CLO, IMI, ACE, MTF, and GLY) by applying  
 194 Eq. 3, then the effect of dissociation on the adsorption of the target chemicals on organic matter was considered  
 195 by using Eq. 4.

$$I = 10^{(pH - pK_a)} \quad \text{Eq. 3}$$

$$K_{OC} = [(I/(I + 1)) \cdot K_{OC \text{ diss}}] + [(1/(I + 1)) \cdot K_{OC \text{ undiss}}] \quad \text{Eq. 4}$$

$$K_{OC \text{ diss}} = 10^{(0.11 \cdot \log K_{OW} + 1.54)} \quad \text{Eq. 5}$$

196 In detail, the organic carbon to water partition coefficient of the undissociated chemical ( $K_{OC \text{ undiss}}$ ) was taken  
 197 from the literature, while  $K_{OC \text{ diss}}$  was estimated from the water/octanol partitioning coefficient ( $K_{OW}$ ) by means  
 198 of Eq. 5, as reported by Franco and colleagues (Franco and Trapp, 2008; Vitale and Di Guardo, 2019) if no  
 199 experimental data was available (Table S2).

200 Furthermore, following the approach reported by Franco and co-workers (Franco and Trapp, 2010), only the  
 201 undissociated form a chemical was assumed able to diffuse through the air-water interface. For this reason, DV  
 202 was calculated using the equations reported in Table 1 and an additional factor ( $1/(I+1)$ ) accounting for the  
 203 target chemical dissociation was added to the water compartment mass balance equation.

204 All input and removal pathways ( $J_i$ ) related to transport and transformation processes are assumed to occur  
 205 simultaneously and instantaneously once a contaminant enters the system. They were calculated as the product  
 206 of each process flow rate ( $D_i$  values,  $mol \cdot Pa^{-1} \cdot h^{-1}$ ) and the relative compartment fugacity ( $f$ ,  $Pa$ ) using the  
 207 equations shown in Table 1 (Mackay, 2001). In particular, we included both sediment burial (for NBn, NBc,  
 208 and SB) and sediment erosion (for CB) (Sommerfreund et al., 2010b) into a sediment loss pathway ( $D_L$ ) to  
 209 permanently remove the contaminant from the system.

210 Then, the results were used to solve the mass balance equations for the water (Eq. 6) and sediment (Eq. 7)  
 211 compartments under a steady-state assumption (i.e. constant emissions, air fugacity, and inflow water fugacity)  
 212 since air fugacity was assumed equal to that of the atmosphere outside the modelled system (Mackay et al.,  
 213 2014).

$$E_W + \left[ \sum f_{i_i} \cdot (D_{I_i} + D_{X_i}) \right] + f_A \cdot (D_V + D_M + D_C + D_Q) + f_S \cdot (D_{RS} + D_T) \\ = f_W \cdot \left( [D_V \cdot (1/(I + 1))] + D_W + D_D + D_T + \left[ \sum (D_{J_i} + D_{Y_i}) \right] \right) \quad \text{Eq. 6}$$

214

$$f_W \cdot (D_D + D_T) = f_S \cdot (D_R + D_T + D_S + D_L) \quad \text{Eq. 7}$$

215 Following the guidelines reported by OECD on overall persistence ( $P_{OV}$ ) and long-range transport potential  
 216 (LRTP) estimation (Gomis et al., 2015; MacKay et al., 2020; OECD, 2020; Whelan, 2013), persistence of the  
 217 selected PPPs in the whole lagoon and in each sub-basin (Eq. 8) was estimated as the ratio of the quantity ( $kg$ )  
 218 of chemical in each region to the respective total rate of loss ( $kg \cdot day^{-1}$ ) from each system, including degradation  
 219 and transport processes. Persistence of the target and sediment pollutants was also investigated separately for  
 220 the water ( $P_W$ ) and sediment ( $P_S$ ) compartments, as shown in Eq. 9 and Eq. 10.

$$P_W = Q_W/J_{W-OUT} = Q_W/(J_{(J+Y)} + J_W + J_V) \quad \text{Eq. 8}$$

221

$$P_S = Q_S/J_{S-OUT} = Q_S/(J_S + J_B) \quad \text{Eq. 9}$$

222

$$P_{OV} = Q_{TOT}/J_{TOT-OUT} = Q_{TOT}/(J_{(J+Y)} + J_W + J_V + J_S + J_B) \quad \text{Eq. 10}$$

223 Where  $Q_W$ ,  $Q_S$ , and  $Q_{TOT}$  represent the quantity of each PPP ( $kg$ ) in the bulk water phase, the bulk sediment  
 224 phase, and in the whole lagoon system at steady state, respectively. Furthermore,  $J_{W-OUT}$ ,  $J_{S-OUT}$ , and  $J_{TOT-OUT}$   
 225 are, respectively, the fluxes ( $kg \cdot h^{-1}$ ) of each PPP out of the bulk water phase, the bulk sediment phase, and out

226 of the whole sub-basin system. In detail,  $J_{W-OUT}$  is composed of the following components: outflow of  
227 dissolved and particle-associated chemical ( $J_{(I+Y)}$ ), volatilization ( $J_V$ ), and transformation ( $J_W$ ). Finally,  $J_{S-OUT}$   
228 is comprised of the selected chemical's outflow due to sediment loss ( $J_L$ ) and transformation ( $J_S$ ). The exchanges  
229 between the water column and the sediment were not included because they do not represent net system losses  
230 (Mackay, 2001; MacKay et al., 2020). Mass balance equations were also used to calculate the predicted  
231 environmental distribution (PED) of the selected PPPs over the different environmental compartments,  
232 following the approach reported by Mackay and co-workers (Daam et al., 2012; Mackay, 2001).

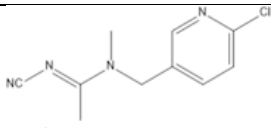
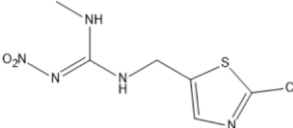
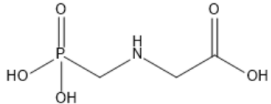
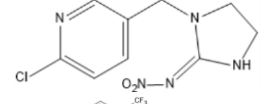
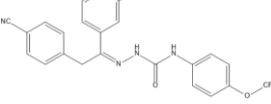
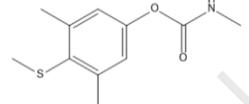
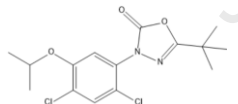
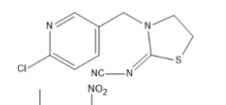
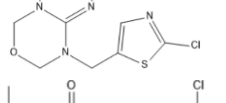
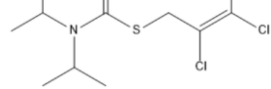
### 233 2.3.2 Model parameters

234 All model parameters including environmental, physical, chemical, and process kinetic ones were selected after  
235 a careful literature review, save for  $C_{IW}$ , which was calculated by model calibration following the approach  
236 described in paragraph 2.2.

237 Environmental parameters (i.e., sediment active layer, sediment solids volume fraction, concentration of  
238 particles in water, organic carbon content of SPM and sediments, sediment deposition/resuspension rate, and  
239 sediment burial/erosion rate) regarding each sub-basin of the Venice Lagoon (i.e. NBn, NBc, CB, and SB) were  
240 taken from Sommerfreund et al. (2010a, b) and calculated as the average of the weighted values according to  
241 the area of each basin's sub-segments. Furthermore, the average SPM concentration (i.e.  $C_{PI}$ ) in each sub-basin  
242 riverine input was calculated as the average of the weighted values according to the discharge of each tributary  
243 using the measurements reported by Collavini *et al.* (2005). No contaminant was assumed to be present within  
244 CB inflow from the sea, and its SPM concentration (i.e.  $9.6 \text{ mg}\cdot\text{L}^{-1}$ ) was taken from ARPAV monitoring data  
245 for the period 2008-2019 (ARPAV, 2019). As reported by Dalla Valle *et al.* (2005b, 2003) dry deposition rate  
246 of atmospheric particulate and organic carbon content of riverine SPM were assumed equal for all basins, and  
247 organic carbon content of SPM flowing from the sea was considered equal to that of the other lagoon inflows.  
248 In detail, the symbols, descriptions, values, and sources of all model inputs values for environmental parameters  
249 are presented in Table S3 and Table S4, while the inputs regarding the selected PPPs chemical properties are  
250 reported in Table 2 and Table S2.

251

252 Table 2: Physico-chemical properties of the selected PPPs. For references and additional information on model parameters see Table S2.

PPP	Structure	Henry's law constant	$K_{OC\_undiss}$	$K_{OC\_undiss}$	Log( $K_{OW}$ )	pKa
		$Pa \cdot m^3 \cdot mol^{-1}$	$L \cdot kg^{-1}$	$L \cdot kg^{-1}$	-	-
Acetamiprid (ACE) CAS: 135410-20-7		9.58E-09	2.67E+02	4.25E+01*	8.00E-01	6.80E-01
Clothianidin (CLO) CAS: 210880-92-5		1.90E-11	5.88E+02	4.36E+01*	9.00E-01	1.11E+01
Glyphosate (GLY) CAS: 1071-83-6		6.94E-08	2.00E+04	1.42E+03	2.00E+04	2.54E+00
Imidacloprid (IMI) CAS: 138261-41-3		1.09E-10	2.93E+02	8.85E+01*	3.70E+00	1.11E+01
Metaflumizone (MTF) CAS: 139968-49-3		1.50E-03	3.38E+04	-	4.60E+00	-
Methiocarb (MTC) CAS: 2032-65-7		9.43E-05	6.60E+02	7.56E+01*	3.08E+00	1.48E+01
Oxadiazon (OXA) CAS: 19666-30-9		1.09E+07	6.76E+02	-	5.33E+00	-
Thiacloprid (TCLO) CAS: 111988-49-9		2.74E-10	6.15E+02	-	1.26E+00	-
Thiamethoxam (TMX) CAS: 153719-23-4		3.56E-10	3.82E+02	-	-1.30E-01	-
Triallate (TRI) CAS: 2303-17-5		8.63E-01	2.94E+03	-	4.06E+00	-

253 \*: Estimated using the approach reported by Franco et al (Franco and Trapp, 2008; Vitale and Di Guardo, 2019).

### 254 2.3.3 Sensitivity and uncertainty analysis on model results

255 The variability in the model predictions due to the uncertainty associated with input values was quantified by  
 256 using the Monte Carlo simulation approach, as already reported by several authors for multimedia fugacity  
 257 model uncertainty analysis (Cao et al., 2004; Kim et al., 2013; Wang et al., 2015, 2020a; Zhang et al., 2013).  
 258 Monte-Carlo analysis (5000 iterations) was used to propagate variance in inputs to the model results (Wang et  
 259 al., 2020a) by applying the Oracle Crystal Ball<sup>®</sup> software (ver. 11.1.2) (Oracle, Redwood City, CA, USA), a  
 260 Microsoft Excel add-on capable of describing each model input as a probability density function, thus  
 261 accounting for both the range of values and the likelihood of the parameter having that value. In detail, all the  
 262 chemical and environmental parameters were assumed to follow a log-normal distribution (Na et al., 2021; Xu  
 263 et al., 2013) and estimated inputs' uncertainty was quantified using confidence factors (*Cfs*), where 95% of  
 264 possible values lie between *Cf* times the median and the median divided by *Cf* (MacLeod et al., 2002). *Cfs*  
 265 values for each input parameter were taken from the literature and are reported in Table S5. The results  
 266 obtained from the uncertainty analysis are reported as coefficients of variation (CVs), calculated as the ratio  
 267 of standard deviation and mean values of a population (Wang et al., 2020b).  
 268 Sensitivity analysis was carried out identify the key input parameters and explore the role of individual  
 269 parameters on the outcome variance of the multimedia model (Cacuci et al., 2003). In some detail, first the  
 270 overall sensitivity was determined by the Spearman rank-order correlation coefficient between the input and  
 271 output data. The individual contribution of each input to the total variance of the outputs (contribution to  
 272 sample variance, CSV) (Tarantola et al., 2012) was estimated as the square of the correlation coefficient  
 273 normalized to the sum of the squared correlation coefficients following the approach reported by Mackay and  
 274 co-workers (Mackay et al., 2014).

### 275 2.3.4 Calibration and evaluation of model performance

276 Data on the measured environmental concentrations (MECs) of the studied PPPs in the case study area were  
 277 available from a recent baseline field study carried out by Pizzini et. al (2024) in the framework of the  
 278 Venezia2021 project and used for model evaluation and calibration.  
 279 In some detail, the work reported by Pizzini and colleagues included four sampling campaigns: spring 2019  
 280 (end of April-beginning of March), autumn 2019 (end of October-beginning of November), summer 2020 (end  
 281 of July-beginning of August), and winter 2021 (end of January-beginning of February). Water and sediment  
 282 samples were collected in six sampling sites, shown in Figure 1b and Table S6. Details on analytical methods,  
 283 results, and sampling procedures are reported in Pizzini et. al (2024).  
 284 Model calibration was performed by using the Oracle Crystal Ball<sup>®</sup> software interfaced with the level III  
 285 fugacity model to locate the parameter value corresponding to the simulation output that best fitted the target  
 286 chemical average measured environmental concentrations (MECs) (Table S8) by automatically varying, in the  
 287 range defined in the literature (Table S5), the value assigned to the selected input (Wang et al., 2020b).  
 288 As reported by several authors, to calculate each PPP average MEC in both water and sediment, the samples  
 289 that were below the limit of detection (LOD) were assigned a value of half of LOD (LOD/2) (Masiá et al.,  
 290 2013). Model calibration was carried out for the PPPs whose average MEC in the water or in the sediments  
 291 exceeded the detection limit and for those chemicals whose PECs exceeded LOD/2 when the corresponding  
 292 MECs were below the detection limit for all the samples.  
 293 Model results were evaluated by comparing each target chemical's average MEC in water (Table S6) and  
 294 sediments (Table S8) with the corresponding PEC estimated by the model according to Eq. 11.

$$PEC/MEC_{PPP} = PEC_{PPP}/MEC_{PPP} \quad \text{Eq. 11}$$

295 In detail, the model results were considered acceptable if the PEC fell within an order of magnitude of the  
 296 MEC (i.e. if the  $PEC/MEC_{PPP}$  ratio ranged between 0.1 and 10) (Lamon et al., 2012) or if the predicted  
 297 concentrations in both water and sediment were less than LOD/2 when the corresponding MECs were below  
 298 the detection limit for all the samples.

## 299 3. Results and discussion

### 300 3.1 Predicted environmental concentrations (PECs), transport, and 301 persistence

302 The concentration in bulk water ( $C_{BW}$ ) sediments ( $C_{BS}$ ) of the target chemicals estimated for each segment of  
303 the Venice lagoon is reported in Figure 2a-b and Table S9.

304

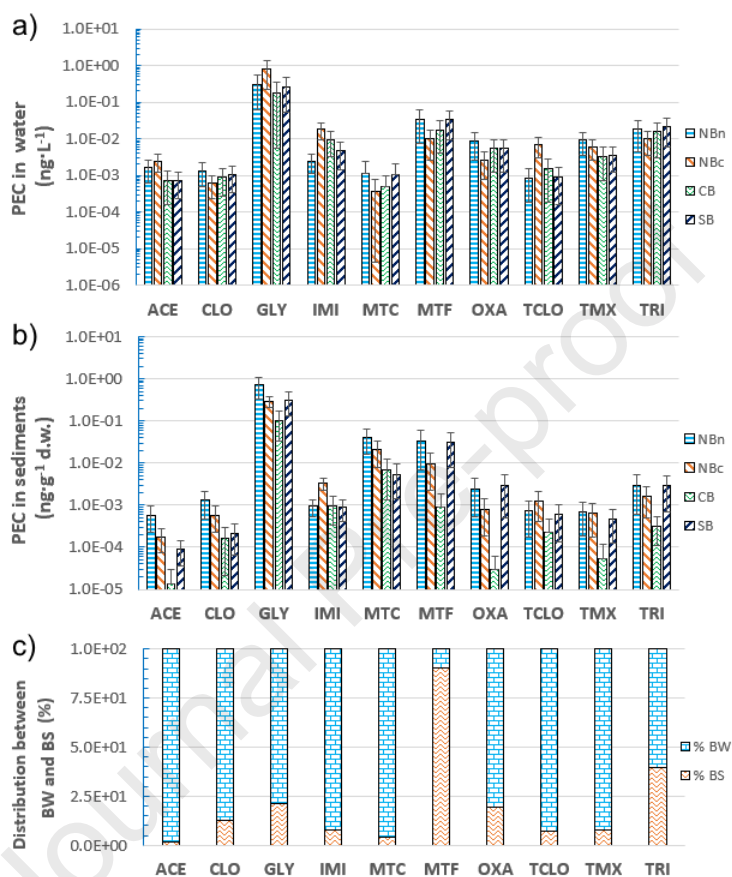


**Figure 2.** Predicted environmental concentrations (PECs) of the selected PPPs in bulk water ( $C_{BW}$ ) (a) and bulk sediment ( $C_{BS}$ ) (b). Distribution of the studied PPPs among bulk sediments (BS) and bulk water (BW) (c). Error bars represent standard deviation of the results.

305

306 Since these estimations reflect a combination of substance properties, emission rates, and lagoon  
307 characteristics, they can be used to obtain important information on the interaction of these chemicals with the  
308 environment. In detail, the results showed remarkable differences in the presence and geographical distribution  
309 of the studied PPP across the lagoon. The model estimated similar concentrations in the water column across  
310 the lagoon for GLY (6-40 ng·L<sup>-1</sup>), TMX, ACE, MTC, TRI, OXA (0.2-2.0 ng·L<sup>-1</sup>), CLO, and MTF (0.02 – 0.1  
311 ng·L<sup>-1</sup>), while the concentration of IMI and TCLO changed more than one order of magnitude between the  
312 different subbasins (0.1- 3.4 ng·L<sup>-1</sup>). In particular, slightly higher levels of TRI, OXA, CLO, and MTF were  
313 estimated for NBn and SB subbasins with respect to the other parts of the lagoon, while for the other PPPs the  
314 highest concentrations in water were obtained for the NBc waterbody. The results reported in Figure 2a-b and  
315 Table S9 show that this spatial distribution could be also found for the sediment compartment, where the  
316 highest concentrations were estimated for GLY (0.2 - 0.8 ng·g<sup>-1</sup> d.w.) and MTF (~ 0.02 ng·g<sup>-1</sup> d.w.). These  
317 trends could be ascribed to both different consumption patterns and transport due to leaching and run-off after  
318 application in the various regions of the lagoon drainage basin, highlighting the importance of improving PPPs  
319 emission estimation methods accounting for soil characteristics, crop type and degradation during transport in  
320 the drainage basin.

321 Furthermore, model results (Figure 2c and Table S10) showed that only a small part of the quantity of ACE,  
322 IMI, MTC, TCLO and TMX discharged into the lagoon would accumulate in the sediments, due to a  
323 combination of several factors such as low affinity to organic matter, high solubility, and persistence in water.  
324 On the contrary, a significant fraction of CLO, GLY, MTF, OXA, and TRI would accumulate in the sediments,  
325 possibly leading to secondary pollution phenomena due to sediment erosion, maintenance of navigable canals  
326 or illegal fishing practices (Dalla Valle et al., 2005a, 2003). This was particularly evident in the case of MTC  
327 due to its fast degradation in the water column and for TRI thanks to a combination of high stability and affinity  
328 to organic matter. This is a very important aspect for the management of the lagoon, especially for the areas  
329 subjected to high inflows of suspended particulate matter either from a tributary or one of the inlets (Zonta et  
330 al., 2020).

331 The average mass transport fluxes of the target chemicals can provide a systematic view on their environmental  
332 behaviour, in particular of the processes involved in their natural attenuation and of the interaction between  
333 the sediments and the overlaying water column (Kong et al., 2018).

334 As can be seen from the results reported in Figure 3a and Table S11, degradation in the water ( $J_w$ ) accounted  
335 for most of the elimination of ACE, CLO, GLY, IMI, MTC, MTF, TCLO, and TMX while transformation in  
336 the sediments ( $J_s$ ) was much more limited, reflecting both their half-lives and distribution within the lagoon  
337 compartments. Considering the several degradation pathways (e.g. oxidation, hydrolysis, photolysis, and  
338 microbial degradation) and products reported for the studied PPPs (e.g. aminomethylphosphonic acid, 6-  
339 chloronicotinic acid, and, 5-dimethyl-4-methylsulfonyl-phenyl-N-methylcarbamate) (Anjos et al., 2021;  
340 Chakraborty et al., 1999; Lopes Catão and López-Castillo, 2018; Pang et al., 2020; Plácido et al., 2013) this  
341 confirms the need for further studies on the presence and effects of their metabolites and degradation products,  
342 as reported by several other authors (Geissen et al., 2015; Tang et al., 2019). Figure 3a shows also that water  
343 outflow ( $J_{J+Y}$ ) contributed significantly to the removal of ACE, CLO, GLY, IMI, MTC, TCLO, and TMX  
344 while volatilization ( $J_v$ ) was a relevant elimination mechanism only in the case of OXA and TRI, due to their  
345 slight volatility and low solubility in water (Comoretto et al., 2008; Yates, 2006). Sediment loss ( $J_l$ ) accounted  
346 only for a small part of the overall loss of the target chemicals, but its contribution to the elimination of the  
347 investigated PPPs with high affinity to organic matter within the CB basin sediments was significantly more  
348 relevant.

349 The transfer fluxes between water and sediments calculated for each PPP are detailed in the Supplementary  
350 Information (Table S12), while Figure 3b shows the net fluxes due to diffusive (i.e.  $J_T$ ) and non-diffusive (i.e.  
351  $J_D$  and  $J_{RS}$ ) processes. As confirmed also by the results on the PPPs' distribution (Figure 2c) there is a net flow  
352 of all chemicals from the water column to the sediments, especially in the case of GLY, MTC, and TRI,  
353 suggesting that the sediment could serve as a sink for these pollutants in the lagoon. Similar trend have already  
354 been reported for other CECs and POPs (Wang et al., 2020b; Xu et al., 2013).

355 The predicted persistence of the target chemicals is reported in Figure 3c and Table S13, showing the longest  
356 overall residence time for MTF (about 6 months) due to its accumulation in the sediments where it is degraded  
357 significantly slower than the other PPPs (Table S2). Similar overall residence times in the water column and  
358 the whole lagoon (about 1-2 months) were estimated for ACE, CLO, GLI, IMI, TMX, TCLO, and TRI,  
359 reflecting the fact that these contaminants have similar water half-lives and were predicted to be for the most  
360 part in the water (Table S2 and Figure 2c). Furthermore, a much shorter stay in the lagoon (about 3-7 days) was  
361 predicted for OXA and MTC due to a combination of limited accumulation in the sediments, rapid  
362 volatilization, and quick degradation in the water (Table S13 and Figure 3). From Figure 3c it can also be seen  
363 that all the studied chemicals exhibited a tendency to remain in the sediments much longer than in the water  
364 column, due to the absence of significant sediment transport and longer half-lives with respect to the water  
365 compartment, indicating a possible risk for benthic organisms (Whelan, 2013). Moreover, PPPs with high  
366 affinity to organic matter showed an estimated persistence in the sediments significantly lower than their  
367 respective degradation half-lives, highlighting the relevance of sediment burial or erosion in their overall  
368 environmental fate.

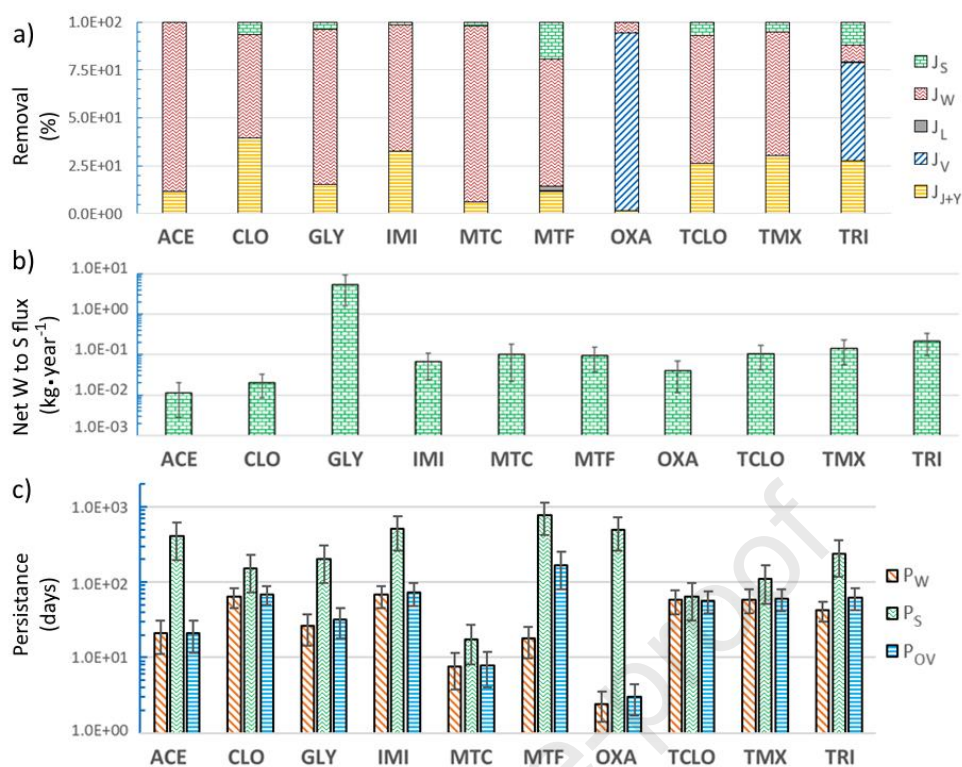


**Figure 3.** Predicted mass transfer fluxes, expressed as a percentage of all loss processes, for the studied PPPs in the Venice lagoon (a). Predicted net transfer fluxes of PPPs across the water–sediment interface in the Venice Lagoon. Positive values indicate net transfer from the water to the sediments. (b). Estimation of the selected PPPs’ persistence in the water column ( $P_W$ ), in the sediments ( $P_S$ ), and in the lagoon ( $P_{OV}$ ) (c). Error bars represent standard deviation of the estimation.

369

### 3.2 Evaluation of model performance

370

371

372

373

374

375

376

377

378

379

380

381

382

383

384

385

386

387

388

389

The model was evaluated by comparing PECs of the PPPs in the water (i.e.  $C_W$ ) and the sediments (i.e.  $C_{BS}$ ) with the arithmetic mean of the measured concentrations detected during the four sampling campaigns (Pizzini et al., 2024), and the results are shown in Figure 4 and detailed in Table S14. In particular, when experimental results above the detection limit were available the agreement between calculated and measured values was always within the acceptable range (i.e.,  $0.1 < \text{PEC}/\text{MEC} < 10$ ), in particular in the case of OXA, ACE, IMI, MTC, and TCLO whose PEC/MEC ratio ranged between 0.3 and 3.0. Furthermore, most of the measurements in the sediments compartment were always below the instrument’s detection limits, therefore it was only possible to conclude that the model did not overestimate the concentration of these contaminants within the sediments. This shows the importance of developing accurate and sensitive analytical methods for the detection of CECs in such matrices, especially in the case of chemicals that have a high affinity for organic matter (Hajeb et al., 2022). For ACE and GLY the model showed a tendency to overestimate their concentration in the water and underestimate it in the sediments (Figure 4 and Table S14), and this could be attributed to an underestimation of their water half-life or of their dissociated form’s affinity to organic matter (Table 2) (Franco and Trapp, 2010; Lamon et al., 2012). From the results reported in Figure 4 and Table S14 it can also be seen that the concentration of CLO and OXA in the water was underestimated in all subbasins except for SB, while the PEC in the sediments was always less than LOD/2, indicating either a possible overestimation of these PPPs’ water half-life or an underestimation of their annual emissions (Kong et al., 2018). These differences between modelled and predicted concentrations could also be ascribed to the inherent simplified nature of the fugacity model with respect to real conditions, for an environment as complex as the Venice Lagoon.

390 For example, the model considers only the annual average concentration and deposition rate of SPM in the  
 391 lagoon, while not accounting for the seasonal variations of zooplankton and phytoplankton's concentration. In  
 392 fact, these factors have been identified as a key factor on the fate and transport of organic pollutants both in  
 393 freshwater and marine environments (Dachs et al., 2000; Kong et al., 2018) due to their influence on air-water  
 394 exchange, sorption, accumulation, and SPM sinking flux (Nizzetto et al., 2012; Tao et al., 2006). The  
 395 integration of the multimedia fate model with an aquatic ecosystem model (Lovato et al., 2013; Pastres et al.,  
 396 2001) accounting for other biotic and abiotic processes may be a solution, but it would greatly increase model  
 397 complexity and the results' uncertainty (Kong et al., 2018).  
 398 Furthermore, more in-depth sampling campaigns would permit to evaluate model results with a more detailed  
 399 spatial discretization of the lagoon, thus deepening our knowledge on the spatial and temporal variability of  
 400 these PPPs distribution in the Venice Lagoon.  
 401

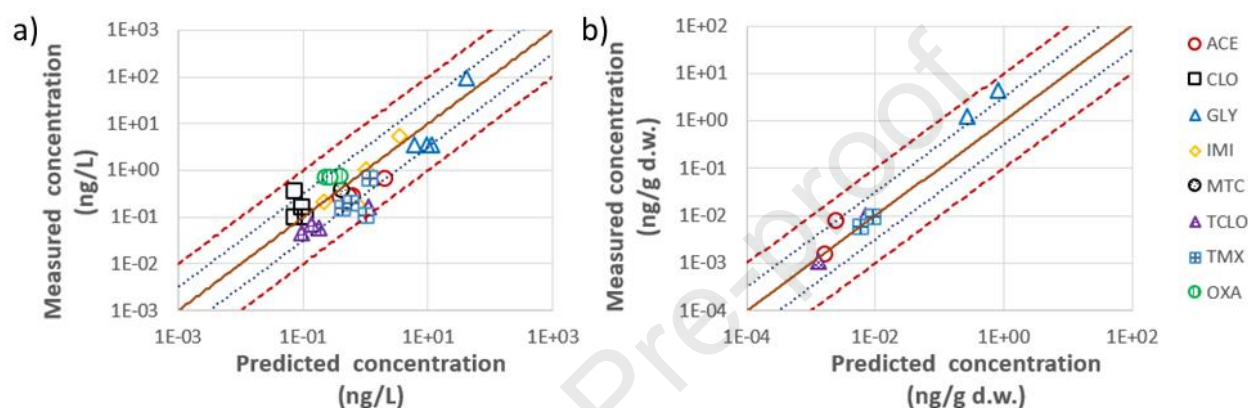


**Figure 4.** Comparisons between the predicted (PEC) and measured (MEC) concentration of the selected PPPs in water ( $C_W$ ) (a) and bulk sediment ( $C_{BS}$ ) (b). Diagonal lines indicate perfect agreement, while the dotted and hatched lines represent agreement within factors of  $10^{0.5}$  and 10, respectively.

### 402 3.3 Sensitivity and uncertainty analysis

#### 403 3.3.1 Sensitivity analysis

404 Model output sensitivity with respect to the concentration of the studied PPPs chemicals in the water and in  
 405 the sediments was investigated and results are reported in Figure 5 and Table S15-S17. The outcomes of  
 406 sensitivity analysis showed that half-life in water accounted for most of the variance (76-92%) attributed to  
 407  $C_{BW}$  for all the studied chemicals, except for TRI and OXA. For the concentration in the water of these two  
 408 chemicals the most important input data were those describing water-air interface processes, and this could be  
 409 ascribed to their higher vapor pressure with respect to the other studied substances (Mackay, 2001). In detail,  
 410 the highest values of CSV for OXA and TRI were shown by the water-side mass transfer coefficient and the  
 411 air-water partitioning coefficient, respectively. This can be related to the value of their Henry's constant,  
 412 showing that the volatilization of OXA is controlled by the processes at the water side of the air-water interface,  
 413 while the volatilization of TRI is controlled by the processes at the air-side (Schwarzenbach et al., 2016). The  
 414 concentration in the water column of the studied PPPs characterized by a high affinity to organic matter (i.e.  
 415 TRI and MTF) was also slightly influenced (CSV  $\approx$  1-3%) by the variation of some of the inputs that describe  
 416 the exchanges between water and sediments, such as  $K_{OC}$ , sediment depth, and resuspension rate. From the  
 417 results reported in Figure 5 and Table S16 it can also be seen that for all the studied PPPs a significant portion  
 418 of the variance attributed to  $C_{BS}$  could ascribed be  $K_{OC}$  (5-25%), sediment porosity (15-30%), and sediment  
 419 density (3-10%) variation. For all PPPs, with the exception of TRI and OXA, a relevant portion (20-60%) of  
 420 the remaining variance attributed to  $C_{BS}$  could be linked to their half-lives in the water, thanks to a combination  
 421 of their higher stability in the sediments with respect to their degradation rate in the water column and their  
 422 limited affinity to organic matter due to dissociation phenomena. In the case of TRI and OXA, similarly to  
 423 what was found for  $C_{BW}$ , a significant contribution to  $C_{BS}$  variance (12 and 40 %, respectively) was given by



424 the mass transfer coefficients describing water-air interface processes. Both the height of the sediments active  
 425 layer and the degradation rate in the sediments contributed to a significant portion (10-20%) of the variance  
 426 attributed to  $C_{BS}$  for those PPPs that are less persistent in the sediments (i.e. MTC, TCLO, TMX, CLO, GLY,  
 427 and TRI), while for the other selected chemicals the contribution of this parameter was much more limited (1-  
 428 5%), highlighting the necessity to accurately estimate the degradation rates of the less stable contaminants (US  
 429 EPA, 2020). The quantity of each chemical discharged into the lagoon of Venice also accounted for a  
 430 significant part of the total variance of  $C_{BW}$  and  $C_{BS}$  (5-12%), showing how the uncertainty linked to this input  
 431 influenced most of the model outputs.

432 The results reported in Figure 5 and Table S17 showed also that the half-life in water of TCLO, CLO, GLY,  
 433 TMX, IMI, MTC, and ACE accounted for most of the variance (90-99%) attributed to  $P_{OV}$  in the lagoon, while  
 434 the most important inputs for estimating TRI and OXA overall persistence (CSV  $\approx$  55-95%) were the mass  
 435 transfer coefficients between water and air. On the contrary, MTF was the only PPP whose residence time in  
 436 the lagoon was significantly influenced by the variation of parameters directly linked to sediments dynamics  
 437 (i.e.  $K_{OC}$ , SedRate, and ReSusRate) due to its low degradation rate in the sediments and high affinity to organic  
 438 matter.

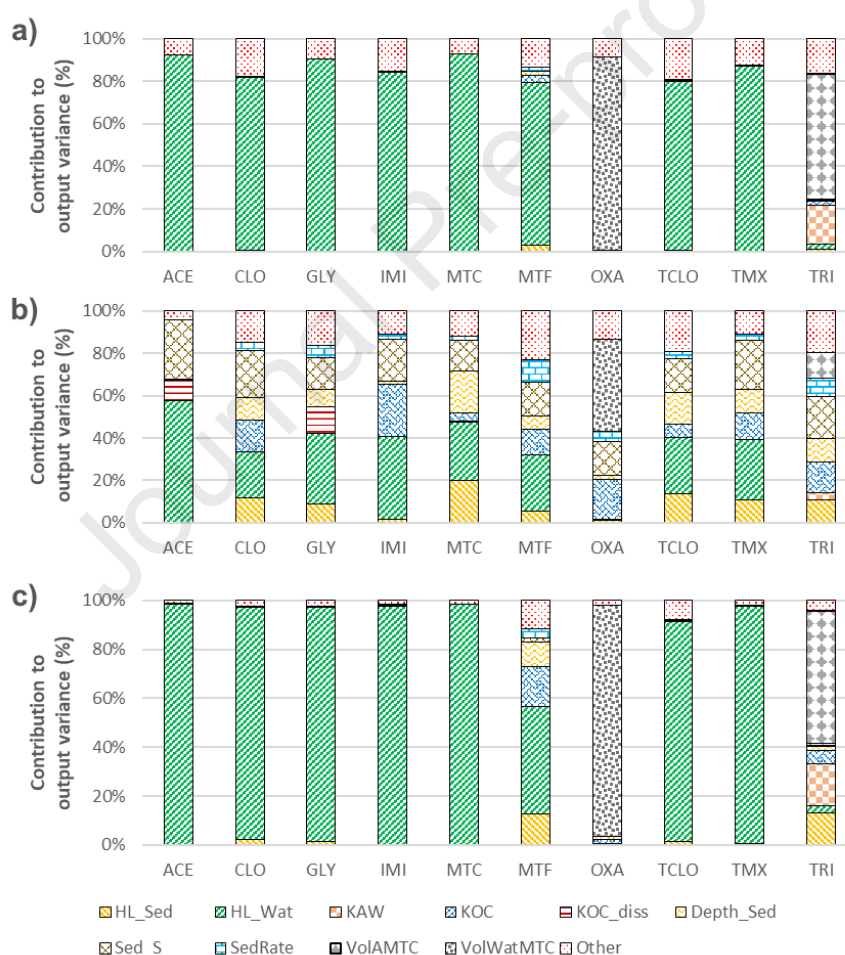


**Figure 5:** Main parameters contributing to CV for the estimation of  $C_{BW}$ ,  $C_{BS}$ , and  $P_{OV}$ . Each value represents the arithmetic mean of the values obtained for each sub-basin.

### 439 3.3.2 Uncertainty analysis

440 Monte Carlo simulation approach was also used to assess model outputs' uncertainty, and coefficients of  
 441 variation (CV) related to  $C_{BW}$ ,  $C_{BS}$ , and  $P_{OV}$  are shown in Figure 6, while the CVs related to other outputs are  
 442 detailed in the Supporting Information (Table S9-S13). There was moderate uncertainty ( $0.20 < CV < 0.40$ )  
 443 for the concentration of the target PPPs in the water compartment, while the CV related to the concentration

444 in the sediments was markedly higher ( $CV > 0.60$ ), due to the contribution of parameters describing sediments'  
 445 dynamics (i.e.  $K_{OC}$ ,  $SedRate$ , and  $ReSusRate$ ). Similarly, there was high uncertainty ( $0.50 < CV < 0.85$ ) also  
 446 for the estimation of studied chemicals' fluxes across the water-sediment interface and out of the system due  
 447 to sediment loss. The uncertainty pertaining the overall persistence of all PPPs, except for MTF, was similar  
 448 to that associated to the estimation of  $C_{BW}$  (Figure 6), reflecting the distribution of these chemicals between  
 449 the environmental media in the lagoon (Figure 2).

450 The high uncertainty related to the model results can also be attributed the high  $Cfs$  (i.e. 3.0) assigned to  
 451 degradation half-lives and active layer sediments depth to account for the scarcity of data on the removal of  
 452 the studied chemicals in brackish waters, such as coastal lagoons and river deltas, and the high re-suspension  
 453 and deposition rates of sediments and SPM in the lagoon (Dalla Valle et al., 2005a).

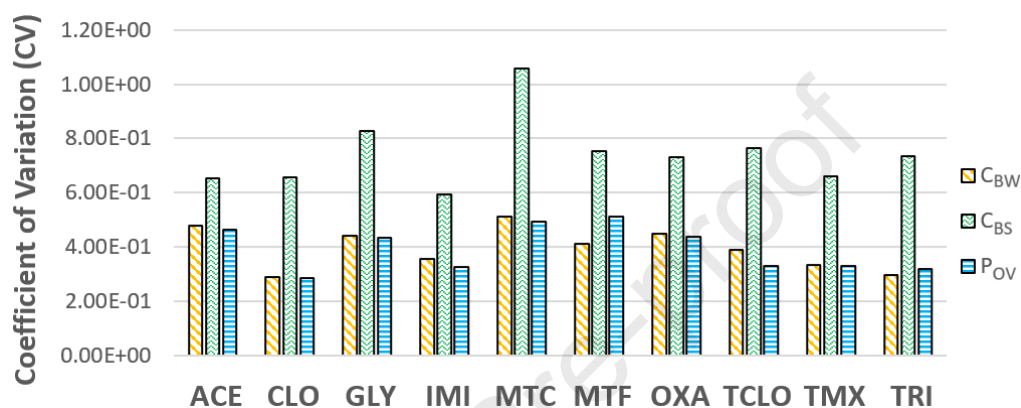


**Figure 6:** Summary of CV values for  $C_{BW}$ ,  $C_{BS}$ , and  $P_{OV}$  for the selected PPPs. Each value represents the arithmetic mean of the values obtained for each sub-basin.

454

### 455 3.4 Strengths, limitations, and implications for environmental risk 456 assessment of the modelling approach

457 The use of level III multimedia fugacity models has been recognized as a suitable tool to support risk  
 458 assessments alongside monitoring studies, as it allows to estimate long-term exposure to chemicals and  
 459 investigate the mechanisms, processes, and emission sources controlling the environmental fate of chemicals  
 460 in complex environments, while requiring a relatively limited amount of information on the modelled system  
 461 (Su et al., 2019). On the contrary, this steady-state modelling approach has been shown to be unsuitable to  
 462 describe the presence of pollution hotspots or sporadic emissions. The use of multimedia fugacity models  
 463 (level IV) assuming unsteady-state distributions and processes (i.e., input rates, mass fluxes, concentrations,  
 464 and fugacity vary with time) was shown to better resolve the presence of such phenomena (Contreras et al.,  
 465 2008; Lu et al., 2024). However, these models require much more specific knowledge on the temporal and  
 466 spatial variation of environmental parameters (e.g., temperature, and SPM concentration) and processes (e.g.,  
 467 water flows, SPM deposition/resuspension, and atmospheric deposition), as well as considerable computing  
 468 resources if high spatial-temporal resolution is required (Guo et al., 2023; Yang et al., 2015)

469 The results of this study offer a first evaluation of the environmental fate and distribution of the selected PPP  
 470 in the Venice Lagoon and highlight the need to further investigate the risks caused by the presence of such  
 471 chemicals and their degradation products in the water and sediments of complex environments like lagoons  
 472 and other brackish water bodies. In fact, the lack of data on the removal of the target PPPs in brackish waters  
 473 accounted for a relevant portion of the overall uncertainty of the model results, indicating the need for more  
 474 studies focused on the degradation of PPPs in such conditions.

475 The modelling exercise carried out in this work also provided valuable insights into the environmental  
 476 processes regulating the fate of the selected PPPs within a complex transitional environment such as the  
 477 Lagoon of Venice.

478 These findings can serve a valuable resource to guide the development of experimental studies focusing on the  
479 degradation of PPP in coastal and transitional environments, as well to support future risk assessments and  
480 investigations focusing on exploring the impact of diverse emission management strategies, such as usage  
481 restrictions or substitution, on the environmental exposure to the studied PPPs and other CECs.

## 482 **4. Conclusions**

483 In this study a level III multimedia fugacity model was applied to simulate the fate and transport of ten PPPs  
484 in a complex coastal lagoon, such as the lagoon of Venice, and the concentration of the selected chemicals  
485 predicted in the water and sediments showed good agreement with field data.

486 The highest concentrations in water were estimated for GLY and IMI, reflecting their high discharge from the  
487 lagoon drainage basin estimated in a previous work (Calgaro et al., 2022). Furthermore, the highest  
488 concentrations in the sediments were predicted for GLY, MTF, and TRI despite the difference of two to three  
489 orders of magnitude of their emissions. Model results also showed a net accumulation in the sediments for all  
490 the studied chemicals, indicating the possibility for sediments to act as sinks for PPPs and, as a consequence,  
491 as secondary source of pollution.

492 The main removal mechanisms for GLY, IMI, ACE, MTC, MTF, TMX, TCLO, and CLO resulted degradation  
493 in the water column and adjective outflow, while volatilization was a key factor for the elimination of OXA  
494 and TRI. Sensitivity and uncertainty analysis highlighted that degradation rates,  $K_{OC}$ , and the parameters  
495 describing air-water interactions had the strongest influence on model's results, followed by the inputs  
496 accounting for sinking and resuspension of sediments.

## 497 **Declaration of competing interests**

498 The authors declare that they have no known competing financial interests or personal relationships that could  
499 have appeared to influence the work reported in this paper.

## 500 **Funding**

501 This study was carried out with the contribution of the "Provveditorato Interregionale Opere Pubbliche per  
502 Veneto, Trentino Alto Adige e Friuli Venezia Giulia" provided through the Consorzio Venezia Nuova and  
503 coordinated by CO.RILA- "Consorzio per il coordinamento delle ricerche inerenti al Sistema Lagunare di  
504 Venezia" within the Venezia2021 project. This study was carried out within the "Interconnected Nord-Est  
505 Innovation Ecosystem (iNEST)" project and received funding from the European Union Next-GenerationEU  
506 - National Recovery and Resilience Plan (NRRP) – MISSION 4 COMPONENT 2, INVESTIMENT N.  
507 ECS00000043 – CUP N. H43C22000540006. This manuscript reflects only the authors' views and opinions,  
508 neither the European Union nor the European Commission can be considered responsible for them.

## 509 **CRedit author statement**

510 **L. Calgaro:** Conceptualization, Methodology, Software, Validation, Investigation, Writing - Original Draft,  
511 Writing - Review & Editing; **E. Giubilato:** Conceptualization, Resources, Data Curation, Writing - Original  
512 Draft, Writing - Review & Editing; **L. Lamon:** Conceptualization, Methodology, Validation, Writing -  
513 Original Draft; **E. Semenzin:** Project administration, Writing - Review & Editing, Methodology, Resources

514

515 **References**

- 516 Anjos, C.S., Lima, R.N., Porto, A.L.M., 2021. An overview of neonicotinoids: biotransformation and  
 517 biodegradation by microbiological processes. *Environ. Sci. Pollut. Res.* 28, 37082–37109.  
 518 <https://doi.org/10.1007/s11356-021-13531-3>
- 519 ARPAV, (Regional Agency for Environmental Prevention and Protection of Veneto [Agenzia Regionale per  
 520 la Prevenzione e Protezione Ambientale del Veneto]), 2019. Coastal marine waters [Acque marino costiere] -  
 521 ARPAV [WWW Document]. URL [https://www.arpa.veneto.it/dati-ambientali/open-data/file-e-](https://www.arpa.veneto.it/dati-ambientali/open-data/file-e-allegati/soaml/nutrienti-e-solidi-sospesi/acque-marino-costiere)  
 522 [allegati/soaml/nutrienti-e-solidi-sospesi/acque-marino-costiere](https://www.arpa.veneto.it/dati-ambientali/open-data/file-e-allegati/soaml/nutrienti-e-solidi-sospesi/acque-marino-costiere)
- 523 Cacuci, D.G., Ionescu-Bujor, M., Navon, I.M., 2003. Sensitivity and Uncertainty Analysis, Volume II:  
 524 Applications to Large-Scale Systems. Chapman & Hall/CRC, Boca Raton, Florida.
- 525 Calgareo, L., Giubilato, E., Lamon, L., Calore, F., Marcomini, A., 2022. Development of an emission inventory  
 526 of contaminants of emerging concern for a coastal lagoon. *Sci. Total Environ.* Submitted.
- 527 Calgareo, L., Giubilato, E., Lamon, L., Calore, F., Semenzin, E., Marcomini, A., 2023. Emissions of  
 528 pharmaceuticals and plant protection products to the lagoon of Venice: development of a new emission  
 529 inventory. *J. Environ. Manage.* 330, 117153. <https://doi.org/10.1016/j.jenvman.2022.117153>
- 530 Calza, P., Medana, C., Padovano, E., Giancotti, V., Minero, C., 2013. Fate of selected pharmaceuticals in river  
 531 waters. *Environ. Sci. Pollut. Res.* 20, 2262–2270. <https://doi.org/10.1007/s11356-012-1097-4>
- 532 Cancelli, A.M., Gobas, F.A.P.C., Wang, Q., Kelly, B.C., 2019. Development and evaluation of a mechanistic  
 533 model to assess the fate and removal efficiency of hydrophobic organic contaminants in horizontal subsurface  
 534 flow treatment wetlands. *Water Res.* 151, 183–192. <https://doi.org/10.1016/j.watres.2018.12.020>
- 535 Cao, H., Tao, S., Xu, F., Coveney, R.M., Cao, J., Li, B., Liu, W., Wang, X., Hu, J., Shen, W., Qin, B., Sun, R.,  
 536 2004. Multimedia Fate Model for Hexachlorocyclohexane in Tianjin, China. *Environ. Sci. Technol.* 38, 2126–  
 537 2132. <https://doi.org/10.1021/es0305860>
- 538 Chakraborty, S.K., Bhattacharya, A., Chowdhury, A., 1999. Degradation of oxadiazon in Kalyani alluvial soil.  
 539 *Pestic. Sci.* 55, 943–948. [https://doi.org/10.1002/\(SICI\)1096-9063\(199909\)55:9<943::AID-PS47>3.0.CO;2-](https://doi.org/10.1002/(SICI)1096-9063(199909)55:9<943::AID-PS47>3.0.CO;2-K)  
 540 [K](https://doi.org/10.1002/(SICI)1096-9063(199909)55:9<943::AID-PS47>3.0.CO;2-K)
- 541 Chang, F., Simcik, M.F., Capel, P.D., 2011. Occurrence and fate of the herbicide glyphosate and its degradate  
 542 aminomethylphosphonic acid in the atmosphere. *Environ. Toxicol. Chem.* 30, 548–555.  
 543 <https://doi.org/10.1002/etc.431>
- 544 Christen, V., Kunz, P.Y., Fent, K., 2018. Endocrine disruption and chronic effects of plant protection products  
 545 in bees: Can we better protect our pollinators? *Environ. Pollut.* 243, 1588–1601.  
 546 <https://doi.org/10.1016/j.envpol.2018.09.117>
- 547 Collavini, F., Bettioli, C., Zaggia, L., Zonta, R., 2005. Pollutant loads from the drainage basin to the Venice  
 548 Lagoon (Italy). *Environ. Int.* 31, 939–947. <https://doi.org/10.1016/j.envint.2005.05.003>
- 549 Comoretto, L., Arfib, B., Talva, R., Chauvelon, P., Pichaud, M., Chiron, S., Höhener, P., 2008. Runoff of  
 550 pesticides from rice fields in the Ile de Camargue (Rhône river delta, France): Field study and modeling.  
 551 *Environ. Pollut.* 151, 486–493. <https://doi.org/10.1016/j.envpol.2007.04.021>
- 552 Contreras, W.A., Ginestar, D., Paraíba, L.C., Bru, R., 2008. Modelling the pesticide concentration in a rice  
 553 field by a level IV fugacity model coupled with a dispersion-advection equation. *Comput. Math. with Appl.*  
 554 56, 657–669. <https://doi.org/10.1016/j.camwa.2008.01.009>

- 555 Daam, M.A., Silva, E., Pereira, A.C.S., Da Silva, L.M.M., Ramos, A.P., Cerejeira, M.J., 2012. Fate and side-  
556 effects of pesticides in urban areas-a case study in Portugal.
- 557 Dachs, J., Eisenreich, S.J., Hoff, R.M., 2000. Influence of Eutrophication on Air–Water Exchange, Vertical  
558 Fluxes, and Phytoplankton Concentrations of Persistent Organic Pollutants. *Environ. Sci. Technol.* 34, 1095–  
559 1102. <https://doi.org/10.1021/es990759e>
- 560 Dalla Valle, M., Marcomini, A., Jones, K.C., Sweetman, A.J., Valle, M.D., Marcomini, A., Jones, K.C.,  
561 Sweetman, A.J., Dalla Valle, M., Marcomini, A., Jones, K.C., Sweetman, A.J., 2005a. Reconstruction of  
562 historical trends of PCDD/Fs and PCBs in the Venice Lagoon, Italy. *Environ. Int.* 31, 1047–1052.  
563 <https://doi.org/10.1016/j.envint.2005.05.015>
- 564 Dalla Valle, M., Marcomini, A., Sfriso, A., Sweetman, A.J., Jones, K.C., 2003. Estimation of PCDD/F  
565 distribution and fluxes in the Venice Lagoon, Italy: combining measurement and modelling approaches.  
566 *Chemosphere* 51, 603–616. [https://doi.org/10.1016/S0045-6535\(03\)00048-1](https://doi.org/10.1016/S0045-6535(03)00048-1)
- 567 Dalla Valle, M., Marcomini, A., Sweetman, A.J., Jones, K.C., 2005b. Temporal trends in the sources of  
568 PCDD/Fs to and around the Venice Lagoon. *Environ. Int.* 31, 1040–1046.  
569 <https://doi.org/10.1016/j.envint.2005.05.014>
- 570 EPPO, (European and Mediterranean Plant Protection Organization), 2003. Environmental risk assessment  
571 scheme for plant protection products. *EPPO Bull.* 33, 115–129. [https://doi.org/10.1046/j.1365-  
572 2338.2003.00621.x](https://doi.org/10.1046/j.1365-2338.2003.00621.x)
- 573 European Commission, 2015. Commission Implementing Decision (EU) 2015/495 of 20 March 2015  
574 establishing a watch list of substances for Union-wide monitoring in the field of water policy pursuant to  
575 Directive 2008/105/EC.
- 576 European Commission, 2000. Directive 2000/60/EC of the European Parliament and of the Council of 23  
577 October 2000 establishing a framework for Community action in the field of water policy. in *Official Journal*  
578 *of the European Union (OJ L) No 327 of 22/12/2000*, pp. 1–73.
- 579 European Commission, 2018. Commission Implementing Decision (EU) 2018/840 of 5 June 2018 establishing  
580 a watch list of substances for Union-wide monitoring in the field of water policy pursuant to Directive  
581 2008/105/EC of the European Parliament.
- 582 Fang, S.-M., Zhang, X., Bao, L.-J., Zeng, E.Y., 2016. Modeling the fate of p,p'-DDT in water and sediment of  
583 two typical estuarine bays in South China: Importance of fishing vessels' inputs. *Environ. Pollut.* 212, 598–  
584 604. <https://doi.org/10.1016/j.envpol.2016.02.052>
- 585 FAO, (Food and Agriculture Organization), ITPS, (Intergovernmental Technical Panel on Soils), 2017. Global  
586 assessment plant of the impact of products protection on soil and soil functions ecosystems. Rome.  
587 <https://doi.org/10.2777/71851>
- 588 Ferrarin, C., Davolio, S., Bellafiore, D., Ghezzi, M., Maicu, F., Mc Kiver, W., Drofa, O., Umgiesser, G., Bajo,  
589 M., De Pascalis, F., Malguzzi, P., Zaggia, L., Lorenzetti, G., Manfè, G., 2019. Cross-scale operational  
590 oceanography in the Adriatic Sea. *J. Oper. Oceanogr.* 12, 86–103.  
591 <https://doi.org/10.1080/1755876X.2019.1576275>
- 592 Franco, A., Trapp, S., 2010. A multimedia activity model for ionizable compounds: Validation study with 2,4-  
593 dichlorophenoxyacetic acid, aniline, and trimethoprim. *Environ. Toxicol. Chem.* 29, 789–799.  
594 <https://doi.org/10.1002/etc.115>
- 595 Franco, A., Trapp, S., 2008. Estimation of the soil-water partition coefficient normalized organic carbon for  
596 ionizable organic chemicals. *Environ. Toxicol. Chem.* 27, 1995–2004. <https://doi.org/10.1897/07-583.1>

- 597 Geissen, V., Mol, H., Klumpp, E., Umlauf, G., Nadal, M., van der Ploeg, M., van de Zee, S.E.A.T.M., Ritsema,  
598 C.J., 2015. Emerging pollutants in the environment: A challenge for water resource management. *Int. Soil*  
599 *Water Conserv. Res.* 3, 57–65. <https://doi.org/10.1016/j.iswcr.2015.03.002>
- 600 Gomis, M.I., Wang, Z., Scheringer, M., Cousins, I.T., 2015. A modeling assessment of the physicochemical  
601 properties and environmental fate of emerging and novel per- and polyfluoroalkyl substances. *Sci. Total*  
602 *Environ.* 505, 981–991. <https://doi.org/10.1016/j.scitotenv.2014.10.062>
- 603 Guo, Y., Wang, C., Huang, P., Li, J., Qiu, C., Bai, Y., Li, C., Yu, J., 2023. A method for simulating spatial  
604 fates of chemicals in flowing lake systems: Application to phthalates in a lake. *Water Res.* 232, 119715.  
605 <https://doi.org/10.1016/j.watres.2023.119715>
- 606 Hajeb, P., Zhu, L., Bossi, R., Vorkamp, K., 2022. Sample preparation techniques for suspect and non-target  
607 screening of emerging contaminants. *Chemosphere* 287, 132306.  
608 <https://doi.org/10.1016/j.chemosphere.2021.132306>
- 609 ISTAT, 2012. Basi territoriali e variabili censuarie - Veneto 2011 [WWW Document]. URL  
610 [http://www.istat.it/storage/cartografia/basi\\_territoriali/WGS\\_84\\_UTM/2011/R05\\_11\\_WGS84.zip](http://www.istat.it/storage/cartografia/basi_territoriali/WGS_84_UTM/2011/R05_11_WGS84.zip) (accessed  
611 12.23.19).
- 612 Kilic, S.G., Aral, M.M., 2009. A fugacity based continuous and dynamic fate and transport model for river  
613 networks and its application to Altamaha River. *Sci. Total Environ.* 407, 3855–3866.  
614 <https://doi.org/10.1016/j.scitotenv.2009.01.057>
- 615 Kim, J., Powell, D.E., Hughes, L., Mackay, D., 2013. Uncertainty analysis using a fugacity-based multimedia  
616 mass-balance model: Application of the updated EQC model to decamethylcyclopentasiloxane (D5).  
617 *Chemosphere* 93, 819–829. <https://doi.org/10.1016/j.chemosphere.2012.10.054>
- 618 Kong, X., Liu, W., He, W., Xu, F., Koelmans, A.A., Mooij, W.M., 2018. Multimedia fate modeling of  
619 perfluorooctanoic acid (PFOA) and perfluorooctane sulphonate (PFOS) in the shallow lake Chaohu, China.  
620 *Environ. Pollut.* 237, 339–347. <https://doi.org/10.1016/j.envpol.2018.02.026>
- 621 Lamon, L., MacLeod, M., Marcomini, A., Hungerbühler, K., 2012. Modeling the influence of climate change  
622 on the mass balance of polychlorinated biphenyls in the Adriatic Sea. *Chemosphere* 87, 1045–1051.  
623 <https://doi.org/10.1016/j.chemosphere.2012.02.010>
- 624 Lopes Catão, A.J., López-Castillo, A., 2018. On the degradation pathway of glyphosate and glycine. *Environ.*  
625 *Sci. Process. Impacts* 20, 1148–1157. <https://doi.org/10.1039/C8EM00119G>
- 626 Lovato, T., Ciavatta, S., Brigolin, D., Rubino, A., Pastres, R., 2013. Modelling dissolved oxygen and benthic  
627 algae dynamics in a coastal ecosystem by exploiting real-time monitoring data. *Estuar. Coast. Shelf Sci.* 119,  
628 17–30. <https://doi.org/10.1016/j.ecss.2012.12.025>
- 629 Lu, Z., Tian, W., Chen, Z., Chu, M., Zhang, S., Liu, B., Zhao, J., Zou, M., Huo, B., Xu, G., 2024. Release of  
630 PAHs from sediments to seawater under wave: Indoor microcosms and level IV fugacity models. *J. Hazard.*  
631 *Mater.* 474, 134799. <https://doi.org/10.1016/j.jhazmat.2024.134799>
- 632 Lupi, L., Bedmar, F., Puricelli, M., Marino, D., Aparicio, V.C., Wunderlin, D., Miglioranza, K.S.B., 2019.  
633 Glyphosate runoff and its occurrence in rainwater and subsurface soil in the nearby area of agricultural fields  
634 in Argentina. *Chemosphere* 906–914. <https://doi.org/10.1016/j.chemosphere.2019.03.090>
- 635 Mackay, D., 2001. *Multimedia Environmental Models: The Fugacity Approach*, Second Edition, 2nd Ed. ed.  
636 CRC Press. <https://doi.org/10.1201/9781420032543>

- 637 MacKay, D., Celsie, A.K.D., Parnis, J.M., Arnot, J.A., 2020. A perspective on the role of fugacity and activity  
638 for evaluating the PBT properties of organic chemicals and providing a multi-media synoptic indicator of  
639 environmental contamination. *Environ. Sci. Process. Impacts* 22, 518–527.  
640 <https://doi.org/10.1039/c9em00496c>
- 641 Mackay, D., Diamond, M., 1989. Application of the QWASI (Quantitative Water Air Sediment Interaction)  
642 fugacity model to the dynamics of organic and inorganic chemicals in lakes. *Chemosphere* 18, 1343–1365.  
643 [https://doi.org/10.1016/0045-6535\(89\)90027-1](https://doi.org/10.1016/0045-6535(89)90027-1)
- 644 Mackay, D., Hughes, L., Powell, D.E., Kim, J., 2014. An updated Quantitative Water Air Sediment Interaction  
645 (QWASI) model for evaluating chemical fate and input parameter sensitivities in aquatic systems: Application  
646 to D5 (decamethylcyclopentasiloxane) and PCB-180 in two lakes. *Chemosphere* 111, 359–365.  
647 <https://doi.org/10.1016/j.chemosphere.2014.04.033>
- 648 Mackay, D., Paterson, S., 1991. Evaluating the multimedia fate of organic chemicals: a level III fugacity  
649 model. *Environ. Sci. Technol.* 25, 427–436. <https://doi.org/10.1021/es00015a008>
- 650 Mackay, D., Paterson, S., Cheung, B., Neely, W.B., 1985. Evaluating the environmental behavior of chemicals  
651 with a level III fugacity model. *Chemosphere* 14, 335–374. [https://doi.org/10.1016/0045-6535\(85\)90061-X](https://doi.org/10.1016/0045-6535(85)90061-X)
- 652 Mackay, D., Paterson, S., Joy, M., 1983a. A quantitative water, air, sediment interaction (QWASI) fugacity  
653 model for describing the fate of chemicals in rivers, *Chemosphere*. [https://doi.org/10.1016/0045-6535\(83\)90125-X](https://doi.org/10.1016/0045-6535(83)90125-X)
- 654
- 655 Mackay, D., Paterson, S., Joy, M., Paterson, S., Joy, M., Paterson, S., Joy, M., Paterson, S., Joy, M., Paterson,  
656 S., Joy, M., 1983b. A quantitative water, air, sediment interaction (QWASI) fugacity model for describing the  
657 fate of chemicals in lakes, *Chemosphere*. [https://doi.org/10.1016/0045-6535\(83\)90251-5](https://doi.org/10.1016/0045-6535(83)90251-5)
- 658 MacLeod, M., Fraser, A.J., Mackay, D., 2002. Evaluating and expressing the propagation of uncertainty in  
659 chemical fate and bioaccumulation models. *Environ. Toxicol. Chem.* 21, 700–709.  
660 [https://doi.org/10.1897/1551-5028\(2002\)021<0700:EAETPO>2.0.CO;2](https://doi.org/10.1897/1551-5028(2002)021<0700:EAETPO>2.0.CO;2)
- 661 MacLeod, M., Scheringer, M., McKone, T.E., Hungerbuhler, K., 2010. The State of Multimedia Mass-Balance  
662 Modeling in Environmental Science and Decision-Making. *Environ. Sci. Technol.* 44, 8360–8364.  
663 <https://doi.org/10.1021/es100968w>
- 664 Masiá, A., Campo, J., Vázquez-Roig, P., Blasco, C., Picó, Y., 2013. Screening of currently used pesticides in  
665 water, sediments and biota of the Guadalquivir River Basin (Spain). *J. Hazard. Mater.* 263, 95–104.  
666 <https://doi.org/10.1016/j.jhazmat.2013.09.035>
- 667 Messing, P.G., Farenhorst, A., Waite, D.T., McQueen, D.A.R., Sproull, J.F., Humphries, D.A., Thompson,  
668 L.L., 2011. Predicting wetland contamination from atmospheric deposition measurements of pesticides in the  
669 Canadian Prairie Pothole region. *Atmos. Environ.* 45, 7227–7234.  
670 <https://doi.org/10.1016/j.atmosenv.2011.08.074>
- 671 Mugnai, C., Giuliani, S., Romano, S., Frignani, M., 2010. Modelling Transfer of Harmful Chemical Within  
672 the Environment : From Inland Urban / Industrial Settlements To Coastal Aquatic Environments, in: CHINA-  
673 ITALY BILATERAL SYMPOSIUM ON THE COASTAL ZONE AND CONTINENTAL SHELF  
674 EVOLUTION TREND. pp. 68–75.
- 675 Na, G., Ye, J., Li, R., Gao, H., Jin, S., Gao, Y., Hou, C., Huang, J., 2021. Fate of polycyclic aromatic  
676 hydrocarbons in the Pacific sector of the Arctic Ocean based on a level III fugacity environmental multimedia  
677 model. *Mar. Pollut. Bull.* 166, 112195. <https://doi.org/10.1016/j.marpolbul.2021.112195>

- 678 Nizzetto, L., Gioia, R., Li, J., Borgå, K., Pomati, F., Bettinetti, R., Dachs, J., Jones, K.C., 2012. Biological  
679 Pump Control of the Fate and Distribution of Hydrophobic Organic Pollutants in Water and Plankton. *Environ.*  
680 *Sci. Technol.* 46, 3204–3211. <https://doi.org/10.1021/es204176q>
- 681 NORMAN, 2020. NORMAN - Network of reference laboratories, research centres and related organisations  
682 for monitoring of emerging environmental substances [WWW Document]. URL [https://www.norman-](https://www.norman-network.net/)  
683 [network.net/](https://www.norman-network.net/) (accessed 3.30.20).
- 684 OECD, (Organisation for Economic Co-operation and Development), 2020. OECD Pov and LRTP Screening  
685 Tool - OECD [WWW Document]. URL [https://www.oecd.org/en/data/tools/screening-tool-for-overall-](https://www.oecd.org/en/data/tools/screening-tool-for-overall-persistence-and-long-range-transport-potential.html)  
686 [persistence-and-long-range-transport-potential.html](https://www.oecd.org/en/data/tools/screening-tool-for-overall-persistence-and-long-range-transport-potential.html) (accessed 11.26.20).
- 687 Pang, S., Lin, Z., Zhang, W., Mishra, S., Bhatt, P., Chen, S., 2020. Insights Into the Microbial Degradation  
688 and Biochemical Mechanisms of Neonicotinoids. *Front. Microbiol.* 11.  
689 <https://doi.org/10.3389/fmicb.2020.00868>
- 690 Pastres, R., Solidoro, C., Cossarini, G., Melaku Canu, D., Dejak, C., 2001. Managing the rearing of Tapes  
691 philippinarum in the lagoon of Venice: A decision support system. *Ecol. Modell.* 138, 231–245.  
692 [https://doi.org/10.1016/S0304-3800\(00\)00404-X](https://doi.org/10.1016/S0304-3800(00)00404-X)
- 693 Pizzini, S., Giubilato, E., Morabito, E., Barbaro, E., Bonetto, A., Calgaro, L., Feltracco, M., Semenzin, E.,  
694 Vecchiato, M., Zangrando, R., Gambaro, A., Marcomini, A., 2024. Contaminants of emerging concern in water  
695 and sediment of the Venice Lagoon, Italy. *Environ. Res.* 249, 118401.  
696 <https://doi.org/10.1016/j.envres.2024.118401>
- 697 Plácido, A., Paíga, P., Lopes, D.H., Correia, M., Delerue-Matos, C., 2013. Determination of Methiocarb and  
698 Its Degradation Products, Methiocarb Sulfoxide and Methiocarb Sulfone, in Bananas Using QuEChERS  
699 Extraction. *J. Agric. Food Chem.* 61, 325–331. <https://doi.org/10.1021/jf304027s>
- 700 Pogăcean, M.O., Gavrilescu, M., 2009. Plant protection products and their sustainable and environmentally  
701 friendly use. *Environ. Eng. Manag. J.* 8, 607–627. <https://doi.org/10.30638/eemj.2009.084>
- 702 Ravier, S., Désert, M., Gille, G., Armengaud, A., Wortham, H., Quivet, E., 2019. Monitoring of Glyphosate,  
703 Glufosinate-ammonium, and (Aminomethyl)phosphonic acid in ambient air of Provence-Alpes-Côte-d’Azur  
704 Region, France. *Atmos. Environ.* 204, 102–109. <https://doi.org/10.1016/j.atmosenv.2019.02.023>
- 705 Schwarzenbach, R.P., Gschwend, P.M., Imboden, D.M., 2016. *Environmental Organic Chemistry - 3rd Ed.*,  
706 3rd Ed. ed. John Wiley & Sons, Incorporated.
- 707 Sharma, S., Bhattacharya, A., 2017. Drinking water contamination and treatment techniques. *Appl. Water Sci.*  
708 7, 1043–1067. <https://doi.org/10.1007/s13201-016-0455-7>
- 709 Şimşek, A., Küçük, K., Bakan, G., 2019. Applying AQUATOX for the ecological risk assessment coastal of  
710 Black Sea at small industries around Samsun, Turkey. *Int. J. Environ. Sci. Technol.* 16, 5229–5236.  
711 <https://doi.org/10.1007/s13762-019-02251-4>
- 712 Solidoro, C., Melaku Canu, D., Cucco, A., Umgiesser, G., 2004. A partition of the Venice Lagoon based on  
713 physical properties and analysis of general circulation. *J. Mar. Syst.* 51, 147–160.  
714 <https://doi.org/10.1016/j.jmarsys.2004.05.010>
- 715 Sommerfreund, J.K., Arhonditsis, G.B., Diamond, M.L., Frignani, M., Capodaglio, G., Gerino, M., Bellucci,  
716 L., Giuliani, S., Mugnai, C., 2010a. Examination of the uncertainty in contaminant fate and transport modeling:  
717 A case study in the Venice Lagoon. *Ecotoxicol. Environ. Saf.* 73, 231–239.  
718 <https://doi.org/10.1016/j.ecoenv.2009.05.008>



- 719 Sommerfreund, J.K., Gandhi, N., Diamond, M.L., Mugnai, C., Frignani, M., Capodaglio, G., Gerino, M.,  
720 Bellucci, L.G., Giuliani, S., 2010b. Contaminant fate and transport in the Venice Lagoon: Results from a multi-  
721 segment multimedia model. *Ecotoxicol. Environ. Saf.* 73, 222–230.  
722 <https://doi.org/10.1016/j.ecoenv.2009.11.005>
- 723 Stefanakis, A.I., Becker, J.A., 2015. A review of emerging contaminants in water: Classification, sources, and  
724 potential risks. *Impact Water Pollut. Hum. Heal. Environ. Sustain.* 55–80. <https://doi.org/10.4018/978-1-4666-9559-7.ch003>
- 726 Su, C., Zhang, H., Cridge, C., Liang, R., 2019. A review of multimedia transport and fate models for chemicals:  
727 Principles, features and applicability. *Sci. Total Environ.* 668, 881–892.  
728 <https://doi.org/10.1016/j.scitotenv.2019.02.456>
- 729 Tan, B.L.L., Hawker, D.W., Müller, J.F., Leusch, F.D.L., Tremblay, L.A., Chapman, H.F., 2007. Modelling  
730 of the fate of selected endocrine disruptors in a municipal wastewater treatment plant in South East  
731 Queensland, Australia. *Chemosphere* 69, 644–654. <https://doi.org/10.1016/j.chemosphere.2007.02.057>
- 732 Tang, Y., Yin, M., Yang, W., Li, H., Zhong, Y., Mo, L., Liang, Y., Ma, X., Sun, X., 2019. Emerging pollutants  
733 in water environment: Occurrence, monitoring, fate, and risk assessment. *Water Environ. Res.* 91, 984–991.  
734 <https://doi.org/10.1002/wer.1163>
- 735 Tao, S., Yang, Y., Cao, H.Y., Liu, W.X., Coveney, R.M., Xu, F.L., Cao, J., Li, B.G., Wang, X.J., Hu, J.Y.,  
736 Fang, J.Y., 2006. Modeling the dynamic changes in concentrations of  $\gamma$ -hexachlorocyclohexane ( $\gamma$ -HCH) in  
737 Tianjin region from 1953 to 2020. *Environ. Pollut.* 139, 183–193.  
738 <https://doi.org/10.1016/j.envpol.2004.12.013>
- 739 Tarantola, S., Kopustinskias, V., Bolado-Lavin, R., Kaliatka, A., Ušpuras, E., Vaišnoras, M., 2012. Sensitivity  
740 analysis using contribution to sample variance plot: Application to a water hammer model. *Reliab. Eng. Syst.*  
741 *Saf.* 99, 62–73. <https://doi.org/10.1016/j.ress.2011.10.007>
- 742 Umgiesser, G., Canu, D.M., Cucco, A., Solidoro, C., 2004. A finite element model for the Venice Lagoon.  
743 Development, set up, calibration and validation. *J. Mar. Syst.* 51, 123–145.  
744 <https://doi.org/10.1016/j.jmarsys.2004.05.009>
- 745 US EPA, (US Environmental Protection Agency), 2020. Guidance to Calculate Representative Half-life  
746 Values and Characterizing Pesticide Degradation [WWW Document]. URL [https://www.epa.gov/pesticide-  
747 science-and-assessing-pesticide-risks/guidance-calculate-representative-half-life-values#current](https://www.epa.gov/pesticide-science-and-assessing-pesticide-risks/guidance-calculate-representative-half-life-values#current)
- 748 Vaz, S.J., 2019. *Sustainable Agrochemistry: A Compendium of Technologies*, 1st ed. ed. Springer  
749 International Publishing. <https://doi.org/10.1007/978-3-030-17891-8>
- 750 Veneto Region, 2020a. Veneto Region technical map [WWW Document]. URL  
751 <https://idt2.regione.veneto.it/idt/downloader/download> (accessed 3.12.20).
- 752 Veneto Region, 2020b. The Geoportal of the Veneto Region - Land Cover Map database 2018 update [II  
753 Geoportale della Regione del Veneto - Banca dati della Carta della Copertura del Suolo aggiornamento 2018]  
754 [WWW Document]. URL  
755 [https://idt2.regione.veneto.it/geoportal/catalog/search/resource/details.page?uuid=r\\_veneto:c0506151\\_CCS2  
756 018](https://idt2.regione.veneto.it/geoportal/catalog/search/resource/details.page?uuid=r_veneto:c0506151_CCS2)
- 757 Veneto Region, 2019. The Geoportal of the Veneto Region [II Geoportale della Regione del Veneto] [WWW  
758 Document]. URL <https://idt2.regione.veneto.it/> (accessed 12.23.21).

- 759 Vitale, C.M., Di Guardo, A., 2019. A review of the predictive models estimating association of neutral and  
760 ionizable organic chemicals with dissolved organic carbon. *Sci. Total Environ.* 666, 1022–1032.  
761 <https://doi.org/10.1016/j.scitotenv.2019.02.340>
- 762 Wang, D.-G., Aggarwal, M., Tait, T., Brimble, S., Pacepavicius, G., Kinsman, L., Theocharides, M., Smyth,  
763 S.A., Alae, M., 2015. Fate of anthropogenic cyclic volatile methylsiloxanes in a wastewater treatment plant.  
764 *Water Res.* 72, 209–217. <https://doi.org/10.1016/j.watres.2014.10.007>
- 765 Wang, Y., Fan, L., Khan, S.J., Roddick, F.A., 2020a. Fugacity modelling of the fate of micropollutants in  
766 aqueous systems — Uncertainty and sensitivity issues. *Sci. Total Environ.* 699, 134249.  
767 <https://doi.org/10.1016/j.scitotenv.2019.134249>
- 768 Wang, Y., Khan, S.J., Fan, L., Roddick, F., 2020b. Application of a QWASI model to produce validated  
769 insights into the fate and transport of six emerging contaminants in a wastewater lagoon system. *Sci. Total*  
770 *Environ.* 721, 137676. <https://doi.org/10.1016/j.scitotenv.2020.137676>
- 771 Warren, C., Mackay, D., Whelan, M., Fox, K., 2005. Mass balance modelling of contaminants in river basins:  
772 A flexible matrix approach. *Chemosphere* 61, 1458–1467. <https://doi.org/10.1016/j.chemosphere.2005.04.118>
- 773 Whelan, M.J.J., 2013. Evaluating the fate and behaviour of cyclic volatile methyl siloxanes in two contrasting  
774 North American lakes using a multi-media model. *Chemosphere* 91, 1566–1576.  
775 <https://doi.org/10.1016/j.chemosphere.2012.12.048>
- 776 Williams, P.D.R.D., Hubbell, B.J., Weber, E., Fehrenbacher, C., Hrady, D., Zartarian, V., 2010. An overview  
777 of exposure assessment models used by the US Environmental Protection Agency, in: *Modelling of Pollutants*  
778 *in Complex Environmental Systems 2*. ILM Publications: United Kingdom, pp. 61–131.
- 779 Xu, F.-L.L., Qin, N., Zhu, Y., He, W., Kong, X.-Z.Z., Barbour, M.T., He, Q.-S.S., Wang, Y., Ou-Yanga, H.L.,  
780 Tao, S., Ou-Yang, H.-L., Tao, S., 2013. Multimedia fate modeling of polycyclic aromatic hydrocarbons  
781 (PAHs) in Lake Small Baiyangdian, Northern China. *Ecol. Modell.* 252, 246–257.  
782 <https://doi.org/10.1016/j.ecolmodel.2012.04.010>
- 783 Yang, M., Khan, F., Garaniya, V., Chai, S., 2015. Multimedia fate modeling of oil spills in ice-infested waters:  
784 An exploration of the feasibility of fugacity-based approach. *Process Saf. Environ. Prot.* 93, 206–217.  
785 <https://doi.org/10.1016/j.psep.2014.04.009>
- 786 Yates, S.R., 2006. Simulating Herbicide Volatilization from Bare Soil Affected by Atmospheric Conditions  
787 and Limited Solubility in Water. *Environ. Sci. Technol.* 40, 6963–6968. <https://doi.org/10.1021/es061303h>
- 788 Zhang, Q.-Q., Zhao, J.-L., Liu, Y.-S., Li, B.-G., Ying, G.-G., 2013. Multimedia modeling of the fate of  
789 triclosan and triclocarban in the Dongjiang River Basin, South China and comparison with field data. *Environ.*  
790 *Sci. Process. Impacts* 15, 2142. <https://doi.org/10.1039/c3em00316g>
- 791 Zonta, R., Cassin, D., Pini, R., Dominik, J., 2020. Substantial Decrease in Contaminant Concentrations in the  
792 Sediments of the Venice (Italy) Canal Network in the Last Two Decades—Implications for Sediment  
793 Management. *Water* 12, 1965. <https://doi.org/10.3390/w12071965>

**Declaration of interests**

The authors declare that they have no known competing financial interests or personal relationships that could have appeared to influence the work reported in this paper.

The authors declare the following financial interests/personal relationships which may be considered as potential competing interests:

Journal Pre-proof